ADVANCED FUNCTIONAL MATERIALS
www.afm-journal.de

Extreme Hydrogel Bioelectronics

Xuecheng He, Dingyao Liu, Binbin Cui, Hao Huang, Shilei Dai, Ivo Pang, Yuchun Qiao, Tailin Xu, and Shiming Zhang**

The last decades have witnessed the rapid growth of hydrogel bioelectronics. Traditional hydrogels face challenges when working under extreme conditions, causing a loss of stabilities and functionalities. This review provides a systematic overview of hydrogels capable of working under extreme conditions, with a focus on their applications in bioelectronic systems. These hydrogels are summarized into categories of anti-mechanical damage, anti-detachment, anti-swelling, anti-freezing, and anti-foreign body response. Strategies including material development and structural design that can endow hydrogels with the above extreme properties are introduced. Finally, current challenges and new opportunities in developing extreme hydrogel bioelectronic devices and systems are discussed.

1. Introduction

Smart bioelectronics have aroused extensive research interest in the past decades and will certainly lead a revolution in peoples' lifestyles.[1,2] Although much progress made, the intrinsic differences between biological tissues and man-made electronics pose challenges that need to be overcome. Hydrogels, as a viscoelastic material composed of hydrophilic polymers with three-dimensional (3D) cross-linked polymer networks, are an ideal candidate for next-generation bioelectronics due to their similarities with biological tissues and versatility in the regulation of their properties.[3–5] The intrinsic soft and flexible properties of hydrogels minimize the mechanical mismatch with biological tissues, and the high water contents of hydrogels provide wet and ion-rich environments. The favorable optionality in the regulation of their electrical and biological properties by physical and chemical strategies also renders hydrogels a unique bridging material to the biological world. These unique merits enable the use of hydrogels into various bioelectronic applications related to soft robotics,[6–8] flexible electronics,[9–11] energy,[12,13] environmental,[14,15] and life science,[16,17] etc.

However, hydrogel-based bioelectronics may encounter various harsh environments in real-world applications (**Figure 1**), which results in a loss of their functions. For example, hydrogel bioelectronics often undergo various mechanical stimuli such as stretching, compression, and bending during their use. These mechanical stimuli can lead to the formation of microcracks and eventually result in the failure of the entire device.[18] Weak affinity between hydrogel bioelectronics and the human body/tissue (in particular, with biofluids) exacerbates the interfacial mismatch. Also, the foreign body response (FBR) should not be ignored, where proteins and cells accumulate around an implanted device and result in the formation of dense fibroblasts, fibrocytes, and collagenous tissue. Consequently, the functionality of the implanted hydrogel-based bioelectronics can be significantly compromised.[19,20] While the swelling behavior of hydrogel is desirable in certain applications, it is often considered a drawback because excessive swelling with volume expansion can cause mechanical instability and reduced interfacial adhesion.[9] Additionally, conventional hydrogels will lose their flexibility, toughness, or conductivity when being frozen at subzero temperatures, greatly limiting the applications of hydrogel-based energy devices for bioelectronics. Extending the feasibility and versatility of hydrogels under extreme environments is thus urgently required to meet the increasing demand in this field.

In this review, we summarize the current strategies to construct extreme hydrogels for bioelectronic applications (**Figure 2**), including anti-mechanical damage, anti-detachment, anti-swelling, anti-freezing, and anti-FBR hydrogels. In each case, we specify how extreme conditions impair the hydrogel's structure or functionality, as well as how different strategies can help mitigate the deterioration. This is followed by a description of the potential bioelectronic applications enabled by these extreme hydrogels. Finally, we discuss the unmet needs and challenges in the development of extreme hydrogel bioelectronics.

X. He, D. Liu, B. Cui, H. Huang, S. Dai, I. Pang, S. Zhang
Electrical and Electronic Engineering
the University of Hong Kong
Hong Kong SAR 999077, P. R. China
E-mail: szhang@eee.hku.hk
T. Xu
The Institute for Advanced Study (IAS)
Shenzhen University
Shenzhen 518060, P. R. China
E-mail: xutailin@szu.edu.cn
Y. Qiao
Huzhou Key Laboratory of Medical and Environmental Applications Technologies
School of Life Sciences
Huzhou University
Zhejiang 313000, P. R. China

The ORCID identification number(s) for the author(s) of this article can be found under https://doi.org/10.1002/adfm.202405896

DOI: 10.1002/adfm.202405896

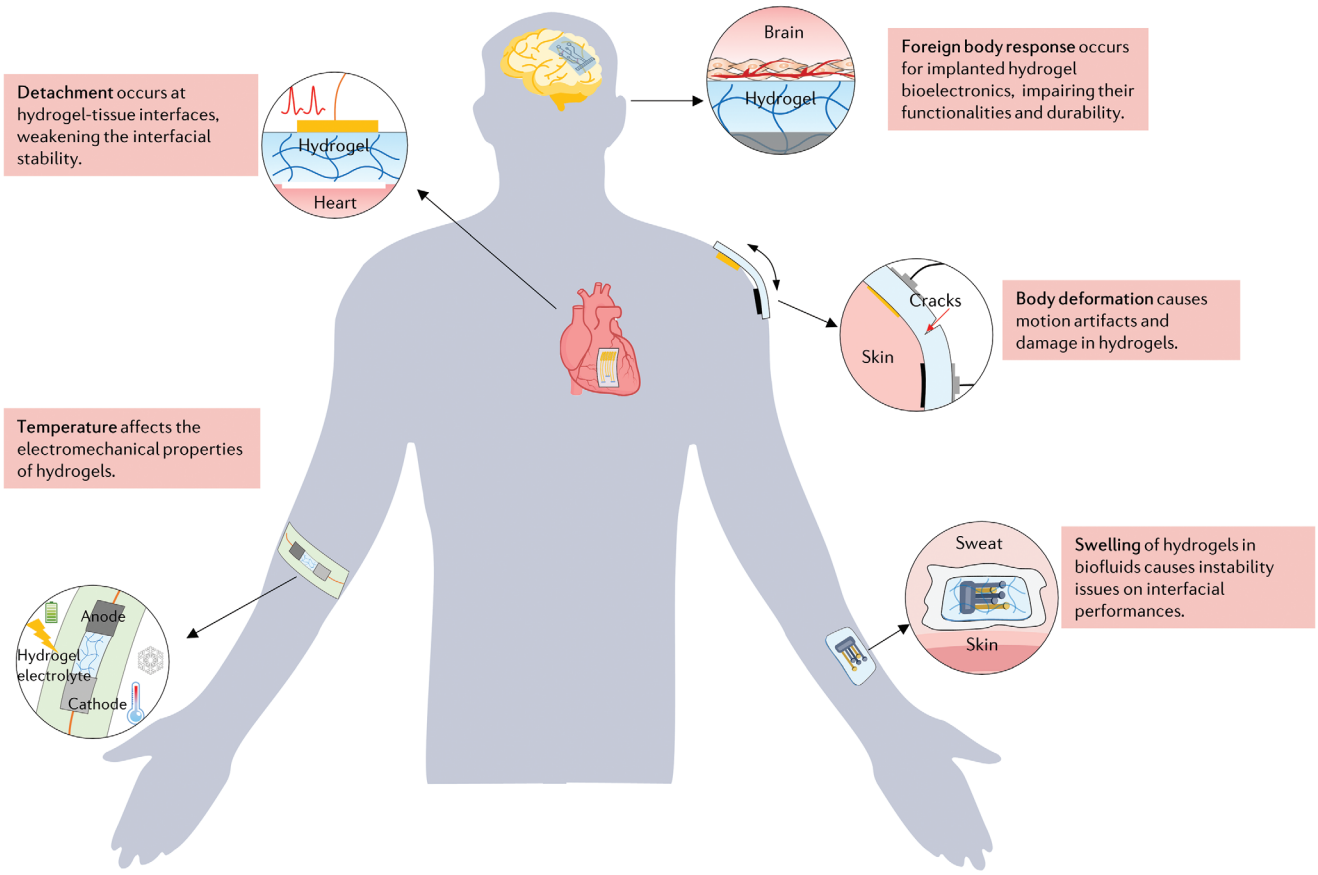

Figure 1. Extreme hydrogel bioelectronics in different scenarios.

2. Anti-Mechanical Damage Hydrogels

Anti-mechanical damage represents superior mechanical performances in the broadest sense, such as high fracture toughness, tensile strength, or fatigue resistance to resist the mechanical damages. Conventional hydrogels typically exhibit poor mechanical performance, for example, with a fracture energy of approximately 10 J m^{-2}, which is significantly lower than that of biological tissues such as heart valves (approximately 1000 J m^{-2}).[26] The design of anti-mechanical damage hydrogels is a basic requirement to minimize the mechanical mismatch issues with biological tissues. Here we summarize three main design strategies of anti-mechanical damage hydrogels including introducing energy dissipation, high-functionality cross-links, and special networks, with a key focus on understanding the fundamental mechanisms of each strategy. Also, self-healing hydrogels capable of recovering mechanical damage are also included.

2.1. Energy Dissipation Mechanism

Energy dissipation is a common strategy employed in the construction of anti-mechanical damage hydrogels. For a conventional hydrogel, the fracture toughness of a polymer network refers to its intrinsic fracture energy Γ_0, corresponding to the covalent energy of a layer of polymer chains per unit area (**Figure** 3a,i). For an anti-mechanical damage hydrogel based on an energy dissipation mechanism, the total fracture toughness is determined by its intrinsic fracture toughness (Γ_0), and the mechanical dissipation (Γ_D) in the process zone ahead of the crack tip. (Figure 3a(ii)). Generally, energy dissipation in this section is performed by incorporating sacrificial regions within the hydrogels. This prevents the cracks from further propagating by effectively dissipating the energy, which can be reflected by the hysteresis loop on its stress-stretch curve under a loading-unloading cycle (Figure 3a(iii)).

Hydrogels with interpenetrating polymer networks have proven to be an effective strategy for energy dissipation. An interpenetrating polymer network is comprised of 2 or more interpenetrated polymer networks, which are individually cross-linked but not joined together. Typical interpenetrating polymer networks can be found in double-network (DN) hydrogels. DN hydrogels can be further classified into three categories: fully chemically cross-linked DN hydrogels, fully physically cross-linked DN hydrogels, and physically-chemically cross-linked DN hydrogels. Compared to single-network hydrogels, DN hydrogels usually exhibit significantly higher fracture toughness. A typical DN hydrogel with full covalent cross-links was proposed in 2003.[27] In this system, one network (poly(2-acrylamido-2-methylpropanesulfonic), PAMPS) consisted of relatively short, stiff, and brittle chains, while the other network (polyacrylamide, PAAm) contained relatively long, coiled, and ductile chains. Both networks are separately cross-linked through covalent bonds. The

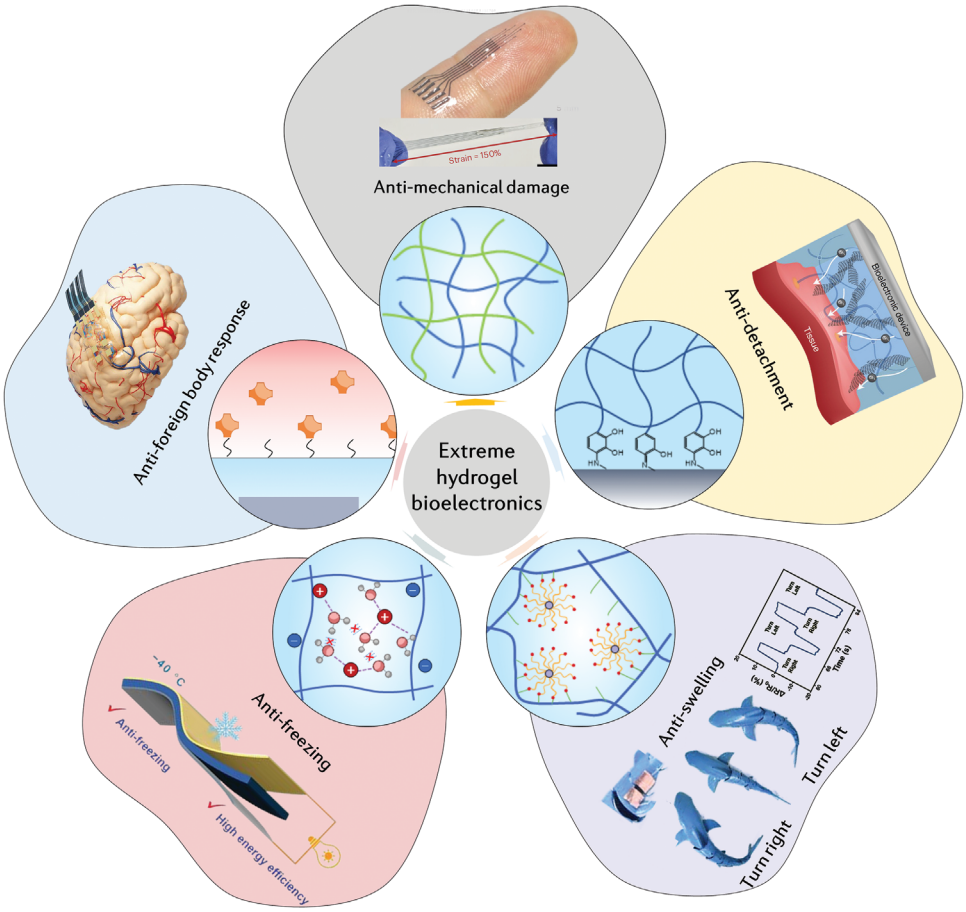

Figure 2. Extreme hydrogel bioelectronics, including anti-mechanical damage (reproduced with permission.[21] Copyright 2023 Springer Nature), anti-detachment (reproduced with permission.[22] Copyright 2021 Springer Nature), anti-swelling (reproduced with permission.[23] Copyright 2023 John Wiley & Sons), anti-freezing (reproduced with permission.[24] Copyright 2022 John Wiley & Sons), and anti-FBR (reproduced with permission.[25] Copyright 2021 Elsevier) hydrogel bioelectronics.

energy dissipation mechanism plays a dominant role in the mechanical reinforcement of this DN hydrogel: when an external force is applied to the DN hydrogel, the short chains are fractured, acting as sacrificial bonds for energy dissipation (Figure 3a(iv)). In contrast, the long ductile networks remain intact, inhibiting crack propagation and maintaining the integrity of the hydrogel. As a result, DN hydrogels can achieve fracture toughness exceeding 1000 J m^{-2}, higher than that of traditional hydrogels (Figure 3a(v)).

DN hydrogels with full covalent cross-links often lack fatigue resistance and recoverable toughness due to the irreversible nature of covalent bonds.[28] To achieve recoverable energy dissipation, several research efforts have been focused on replacing sacrificial covalent bonds with non-covalent interactions, such as electrostatic interactions,[29] hydrogen bonds (H-bonds),[30] hydrophobic associations,[31] etc. These non-covalent bonds with relatively lower binding energies act as sacrificial bonds that break to dissipate mechanical energy under stress. In contrast, the covalent bonds with higher binding energies remain intact, contributing to the stability and toughness of the network. One notable example of a DN hydrogel based on physical and chemical cross-links was proposed in 2012 by Suo's group.[32] The hydrogel was composed of ionically cross-linked alginate and covalently cross-linked PAAm. When the hydrogel was subjected to stress, the alginate chains connected by ionic cross-links broke to dissipate energy, but they could reform when the force was released. On the other hand, the PAAm chains connected by covalent cross-links remained intact. This hydrogel demonstrated exceptional toughness, with the ability to be stretched beyond 20 times its initial length, and exhibited fracture energies of 9000 J m^{-2} (Figure 3a(iv)).

Fully physically cross-linked networks can withstand stress and dissipate energy in a more recoverable manner.[33] These hydrogels rely on a broad distribution of binding strengths of physical cross-links, where weaker cross-links act as sacrificial units while stronger ones maintain the overall integrity of the material.[34] In addition to the DN design, researchers have also explored triple-network hydrogels with multiple interpenetrating polymer networks based on a similar energy dissipation mechanism.[35] Taking inspiration from the hypertrophy and strengthening of human muscles after repeated exercise, a mechanoresponsive hydrogel with a triple network was proposed using a self-growing strategy.[36] Mechanical stress was loaded to break the brittle network of DN hydrogel, generating mechanoradicals at the broken ends of the brittle network strands. Polymerization of monomers

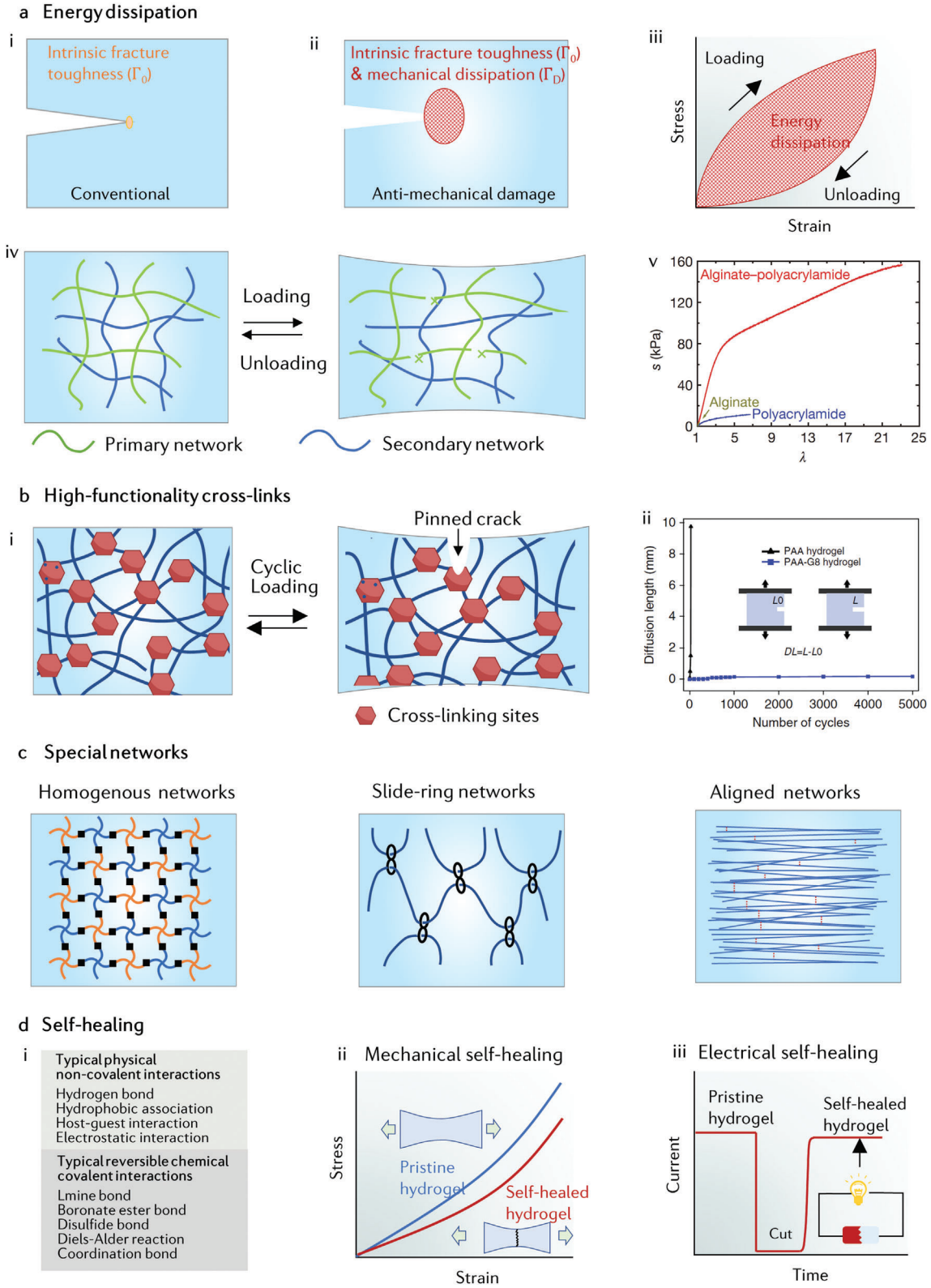

Figure 3. Anti-mechanical damage hydrogels. a) Energy dissipation mechanism. Part i-iii, strategies to increase the fracture energy of traditional hydrogels. Part iv-v, anti-mechanical damage hydrogels based on DN structure. Reproduced with permission.[32] Copyright 2012 Springer Nature b) Anti-fatigue hydrogels based on high functionality cross-links. Reproduced with permission.[37] Copyright 2020 Springer Nature. c) Anti-mechanical damage hydrogels based on special networks including homogenous networks, slide-ring networks, and aligned networks. d) Strategies towards self-healing hydrogels.

from the external solutions was then triggered to form a new third network and further enhanced the mechanical toughness.

Dual-cross-linked (DC) hydrogels typically involve the incorporation of covalent cross-links and noncovalent cross-links within the networks. The DN hydrogels based on physical-chemical cross-links mentioned earlier can be considered a type of DC hydrogel. Additionally, DC hydrogels can be constructed by introducing the covalent and noncovalent cross-links into a single polymer network, resulting in single-network DC hydrogels.[38] Multiple interactions can be employed in the two cross-links to confer specific functionalities to the hydrogel.[16] During loading, reversible noncovalent cross-links act as sacrificial units to dissipate energy at low strains, while the covalent cross-links resist deformation, following a similar energy dissipation mechanism as DN hydrogels.[39] As a result, single-network DC hydrogels exhibit improved mechanical performances, such as stretch strength and fracture toughness, compared to single-cross-linked hydrogels.[40]

2.2. High-Functionality Cross-Links

The functionality is an important parameter that describes the number of polymer chains interconnected at the cross-links. The use of high-functionality cross-links in hydrogels can lead to decoupled mechanical properties. Hydrogels with high-functionality cross-links usually exhibit fine resistance to fracture and in particular, fatigue resistance. Wearable and implantable bioelectronics inevitably face fatigue failure due to continuous mechanical stimuli. Mechanisms for reversible energy dissipation, like fracturing polymer chains in the process zone, are often depleted under cyclic loads, unable to recover in time to resist fatigue crack propagation in subsequent load cycles. To address this issue, the strategy for anti-fatigue hydrogels involves pining the fatigue cracks by high-functionality high-energy phases.[41] In this context, we will summarize high-functionality crystalline domains, macromolecular microspheres, and nanocomposites in hydrogels (Figure 3b(i)).

Crystalline domains in hydrogels serve as strong physical cross-links that connect amorphous polymer chains. The energy required to extract a polymer chain from a crystalline domain is significantly higher than that required to damage the chain itself.[42] As a result, the presence of crystalline domains in hydrogels can greatly enhance their mechanical performances, particularly in terms of fatigue strength. Macromolecular microsphere composite hydrogels are a type of tough hydrogel in which macromolecular microspheres serve as the cross-links.[43] These macromolecular microspheres (e.g., functionalized polystyrene,[44] chitosan microspheres)[45] possess numerous binding sites on their reactive surfaces, allowing for the connection of numerous long polymer chains with controllable cross-link densities. An anti-fatigue poly(acrylic acid) (PAA) hydrogel was achieved by utilizing polyproteins as macromolecular cross-linkers. These polyproteins can unfold to resist crack propagation in the fracture zone when subjected to external forces. Remarkably, even after 5000 cycles, no crack propagation was observed in the hydrogel, demonstrating its excellent anti-fatigue properties (Figure 3b(ii)).[37] The introduction of nanocomposites also enables the formation of high-functionality cross-links for anti-mechanical damage hydrogels.[46,47] Various types of nanomaterials can be introduced into hydrogel including 0D, 1D, 2D nanocomposite.[46] These nanomaterials can produce physical or chemical interactions with the polymer chains, providing redistribution and resistance of applied loads within the hydrogel networks and preventing macroscopic crack propagation.[48] In addition to enhancing mechanical properties, the incorporation of functional nanocomposites in hydrogels can also improve anti-freezing performance (will be discussed later),[44] and conductivity for bioelectronic applications.[49]

2.3. Special Networks

Beyond the above strategies, some special polymer networks have also been proposed to construct anti-mechanical damage hydrogels, including a homogenous network,[50] slide-ring network,[51] and aligned network (Figure 3c).[52,53] Due to the ultralow structural defect, homogeneous network hydrogels usually exhibit high stretchability and fracture toughness. The slide-ring networks allow for the reconfiguration of polymer chains and the equalization of tension within a single polymer chain and among adjacent polymers, forming relatively homogenous polymer networks. For aligned network hydrogels, the enhanced anti-mechanical damage performances can be attributed to the align-induced high strength.

2.4. Self-Healing

While anti-mechanical damage strategies are commonly used in hydrogel bioelectronics, long-term usage can still lead to mechanical damage. Wound healing in organisms offers an inspiration to impart hydrogel bioelectronics with “self-regeneration” or “self-healing” capabilities. The self-healing capability is crucial in soft bioelectronics as it can address structure fracture and function failure or degradation during operation. Here, we focus on intrinsic self-healing hydrogels, which do not require external stimuli for their self-healing behavior. These hydrogels possess the ability to reconstruct their broken bonds after damage, thereby restoring their original mechanical, chemical, and electrical properties. During the self-healing process, the spontaneous recovery of polymer chains with reactive chain ends is based on reversible interactions, including reversible chemical covalent interactions and physical noncovalent interactions (Figure 3d(i)).[54] These reversible interactions undergo dissociation and recombination, enabling the hydrogels to heal damages and regain comparable mechanical and electrical performances. Reversible covalent chemistry plays a crucial role in the development of self-healing hydrogels. Typical reversible covalent bonds for self-healing hydrogels include imine bonds, boronate ester bonds, Diels-Alder (DA) reactions, disulfide bonds, etc.[55] Self-healing hydrogels can also be formed based on non-covalent physical interactions, including H-bonds, hydrophobic associations, host-guest interactions, electrostatic interactions, etc.[56] Each interaction has its own characteristic, and the researchers can choose the proper one regarding the specific components of hydrogels.

The purpose of self-healing design is to recover the structure and functionality of hydrogels. Self-healing efficiency is an

important parameter and is usually determined by comparison of specific performances (such as stress-strain characteristics, Figure 3d(ii)) before and after self-healing. For conductive hydrogels, structural self-healing properties can contribute to electrical self-healing. During the self-healing process, the electrically percolating pathways reform accompanied by conductive component recontact (Figure 3d(iii)).[57,58] The distribution of conductive composite has an important impact on the electrical performance self-healing efficiency. Aligned carbon nanotubes (CNTs) in hydrogel have proven to facilitate low resistance and high electrical self-healing behavior for conducive hydrogel.[59] When two fractured segments of the hydrogel composite are contacted, the aligned CNTs could autonomously recover the electrical conductivity.

3. Anti-Detachment Hydrogels

A stable interface is fundamental for the deployment of hydrogel bioelectronic devices. This necessitates robust bonding (anti-detachment) between the electrical sensing surface and the tissue. However, delamination of bioelectronics from the skin or biological tissues can disrupt stimulation or consistency in recording biological signals and introduce noise to recorded signals. Anti-detachment hydrogels, with strong adhesion to target substrates, are anticipated to overcome this challenge. The anti-detachment hydrogel systems rely on two main components (**Figure** 4a): a tough hydrogel that can dissipate mechanical forces in the vicinity of the detachment zone (Γ_D^{inter}), and strong interfacial linkages between the hydrogel and the targeted substrate (Γ_0^{inter}).[60] The tough hydrogel prevents crack propagation within the hydrogel itself, ensuring that cohesive failure does not occur during the detachment process. To achieve strong interfacial linkages, strategies are employed to prevent crack propagation at the hydrogel-substrate interface and avoid adhesive failure. As we have already discussed the tough hydrogel materials earlier, this section will focus on the methods used to create robust interfacial linkages at the hydrogel-substrate interface.

3.1. General Approaches

Robust hydrogel-substrate interfacial linkages can be achieved through several general interfacial linkage techniques, including physical attachment, chemical anchorage, primer interpenetration, and mechanical interlocked structure (Figure 4b). Physical attachment techniques rely on high-density physical interactions (i.e., crystalline domains,[42] H-bonds,[61] electrostatic interactions).[62] Physical bonding is very facile without complex procedures. Nevertheless, pure physical bonding usually suffers from relatively low bonding strength. Chemical bonding relies on the formation of covalent bonds between functional groups present in the hydrogel and the substrate. Inspired by the natural adhesive proteins in mussels, catechol derivatives are widely used to generate strong both chemical covalent and physical non-covalent bonds between anti-detachment hydrogels and the substrates.[63] Zhao's group used a silane coupling agent, namely, (3-trimethoxysilyl) propyl methacrylate (TMSPMA) to modify into polymer chains via copolymerization, which could be further hydrolyzed into silanol.[64] Then silanol groups condensed with each other to cross-link the polymer chains and condensed with the hydroxyl groups on the substrate to chemically interlink the polymer network onto the targeted substrate.[65] Generally, chemical covalent anchorages offer higher bonding strength for long-term applications compared to physical attachments. However, potential risks associated with added chemicals need to be carefully considered. Additionally, interfacial entanglements by introducing anchoring primers is also an effective adhesion strategy, exhibiting versatility in bonding hydrogel-hydrogel, hydrogel-elastomer, and hydrogel-tissue interfaces.[66] The anchoring primers are limited in low diffusion and permeation toward the substrate, which usually requires external stimuli. Ultrasound, for example, can push the anchoring primers into biological tissues at greater depths by microbubble cavitation, enabling tough bio adhesion with precise control.[67] Mechanically interlocked structures enable high interfacial toughness by increasing the interfacial area and employing locked snap-fits at the hydrogel-substrate interface. Substrates can be designed with porous or groove shapes, allowing the hydrogels to infuse and establish strong interpenetrating adhesion.[68,69] While mechanically interlocked structures offer effective and robust adhesion, they require sophisticated microfabrication techniques, which can increase manufacturing complexity and costs.

3.2. Underwater Approaches

The interfacial toughness of hydrogels is particularly crucial in underwater working environments. Hydrogels tend to form a hydration layer at the interface due to the strong hydration behavior of hydrophilic polymer chains, which significantly weakens the interfacial toughness. While some catechol-derived hydrogels can provide an intrinsic robust anti-detachment performance even in the presence of a hydration layer,[70] there is still a need to enhance underwater interfacial toughness by disrupting the hydration layer (Figure 4c). One effective strategy is to absorb the hydration layer using hygroscopic materials through in situ gelation.[71–73] For example, a hydrogel-based dried double-sided tape has been developed to remove interfacial water from wet substrates, leading to rapid and temporary cross-links at the interface.[74] Using a hygroscopic powder adhesive that can quickly transform into a hydrogel by absorbing interfacial moisture and diffusing into the substrate, forming interpenetrating adhesion.[75] These dehydrating strategies are applicable not only for underwater adhesion but also for adhesion to wet tissues.[76] Creating surface microstructures is another effective strategy. Different from the above-mentioned interlocked microstructures, these microstructures typically consist of interconnected valleys and peaks, inspired by natural organisms such as clingfish discs,[77] and tree frog pads.[78] In contrast to hygroscopic strategies that involve removing interfacial water by absorbing it into the hydrogel's inner space (the gel is relatively dry in its initial state), these microstructures are designed to expel water when applying pressure. Additionally, pushing out the water can create a negative pressure between the interconnected valleys and the targeted substrate, further enhancing the anti-detachment effect.

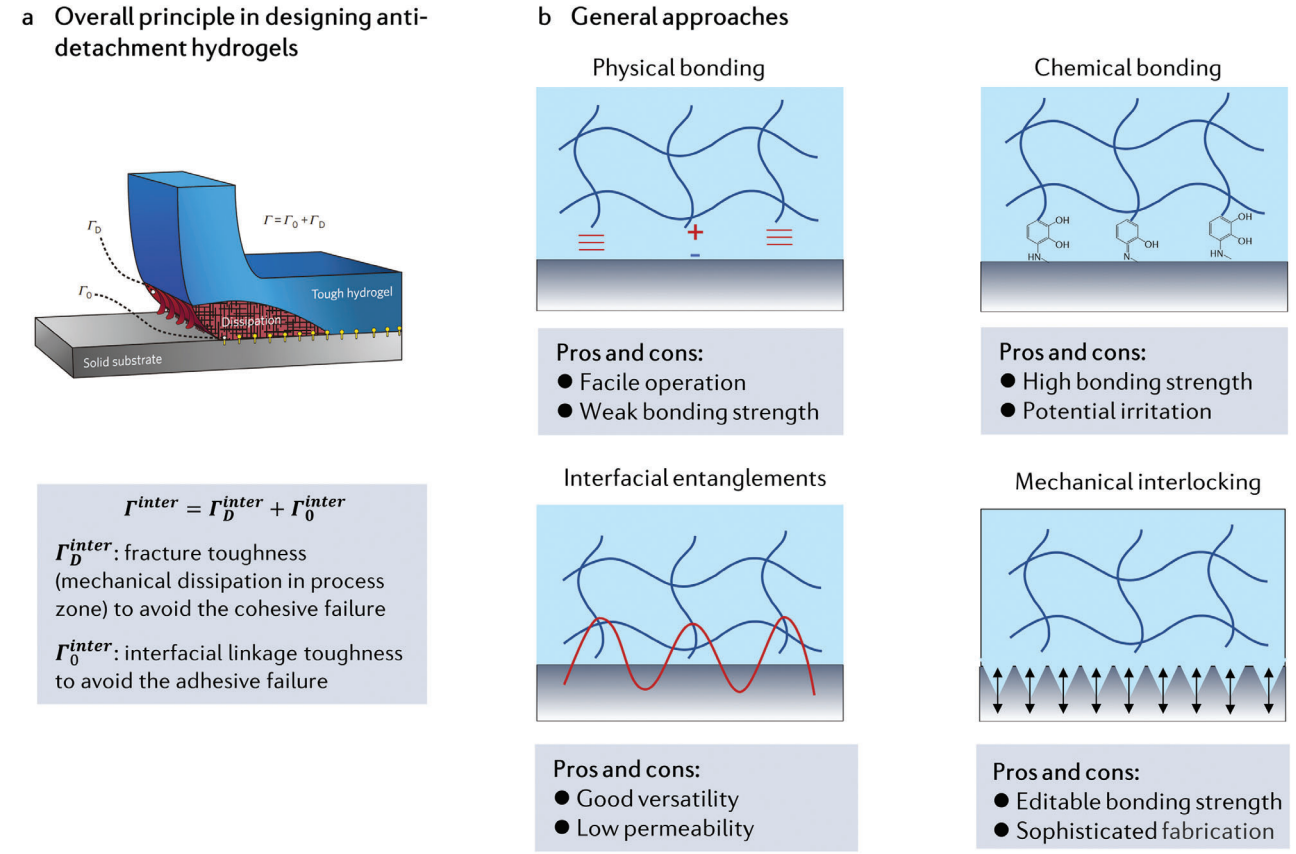

Figure 4. Anti-detachment hydrogels. a) Overall principle in designing anti-detachment hydrogels. Reproduced with permission.[64] Copyright 2016 Springer Nature. b) Anti-detachment hydrogels using general approaches based on physical bonding, chemical bonding, interfacial entanglements, and mechanically interlocked structures. c) Strategies towards underwater anti-detachment hydrogels such as introducing hygroscopic materials and bioinspired microstructures.

4. Anti-Swelling Hydrogels

While swelling behavior is desirable in certain applications, such as superabsorbent materials, it is often considered a drawback because excessive swelling and volume expansion can damage the cross-linked networks and weaken the functionality of the hydrogel, including mechanical instability, interfacial mismatch, and reduced interfacial adhesion. Swelling is a competitive process between the volume expansion and the resistive force of the hydrogel networks. Volume expansion originates from the polymer-water interactions,[79] and the resistive force usually arises from the elastic retractive force exerted by the network chains. At the beginning of the swelling, the volume expansion prevails over the elastic retractive force of hydrogels. As the network chains change from coil conformation to extended conformation progressively with swelling, the elastic retractive force increases continually due to the hydrogel expansion. Thus, the general design principle for anti-swelling hydrogels is to enhance the retractive force and weaken the volume expansion, as demonstrated in **Figure 5a**.

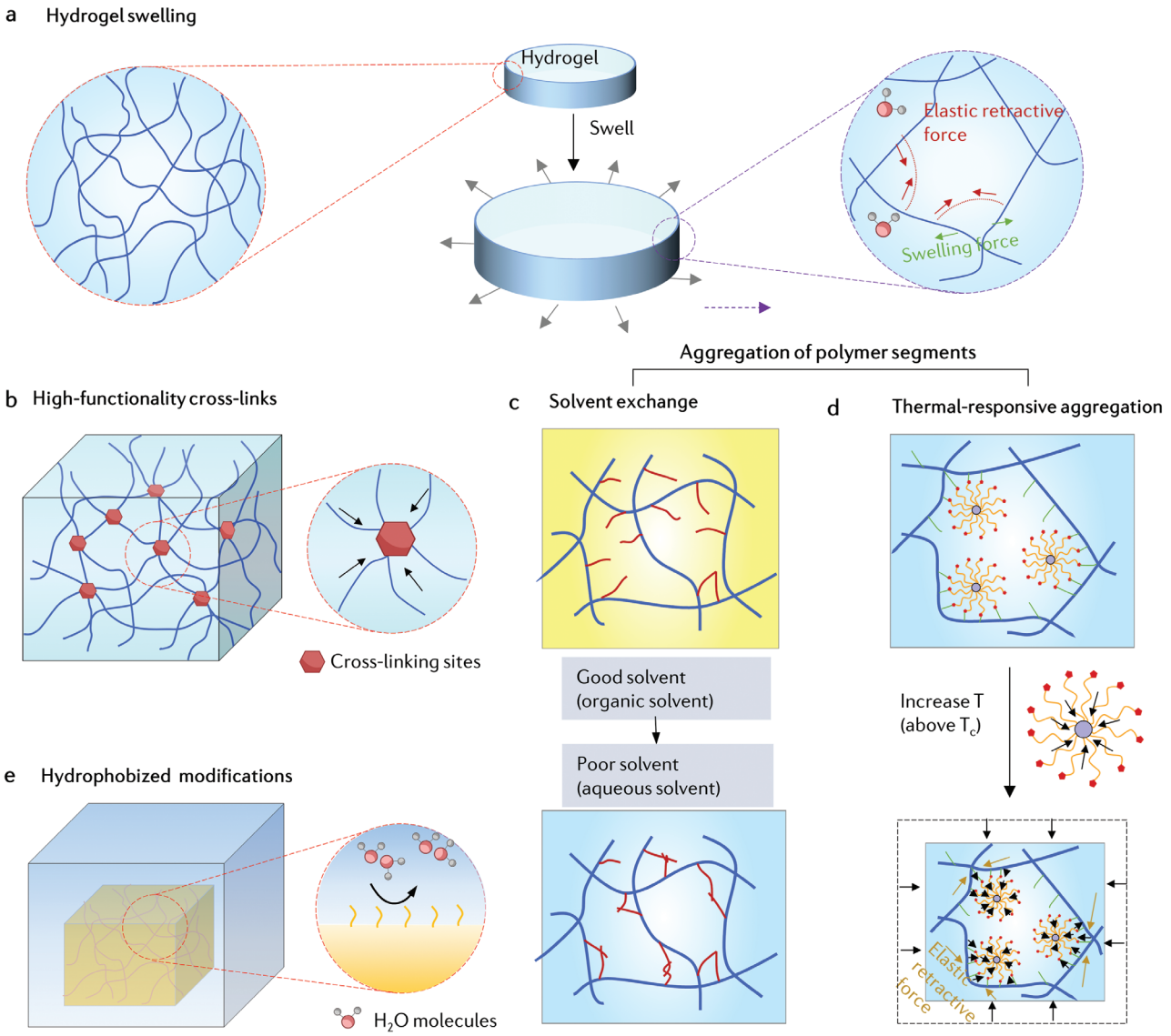

Figure 5. Anti-swelling hydrogels. a) The schematic process of hydrogels. b) Anti-swelling hydrogels based on high-functionality cross-links. c) Anti-swelling hydrogels based on the solvent displacement strategy. d) Anti-swelling hydrogels based on thermal-responsive aggregation. e) Hydrophobized modifications towards anti-swelling hydrogels.

4.1. High-Functionality Cross-Links

Many strategies used to construct anti-mechanical damage hydrogels can indeed be applied to improve the anti-swelling performance of hydrogels. This is because these strategies can maintain the integrity of the hydrogel networks and resist external forces, including mechanical force as well as swelling force. For example, DN hydrogels typically exhibit lower swelling compared to single-network hydrogels.[80] By introducing a hydrophobic second network, the swelling ratio can be further reduced to 20–60%.[81] Additionally, high-functionality cross-links are beneficial for limiting the swelling behavior of hydrogels (Figure 5b). This is because increasing the functionality of cross-links can increase the elastic retractive force to some extent.[61] Typically, a supramolecular hydrogel based on diverse physical interactions (including electrostatic interaction, H-bonds, and hydrophobic associations) was prepared with densely cross-linked networks and good swelling resistance.[82] High-functionality cross-links based on nanocomposites or macromolecular composites can also be used to construct anti-swelling hydrogels. For example, silica particles can impart superior strength and negligible swelling (as low as 2%) to polyvinyl alcohol (PVA) hydrogels in deionized water.[83]

4.2. Aggregation of Polymer Segments

Controlling the aggregation of polymer segments through solvent displacement or temperature changes can counteract the swelling tendency of hydrogels. In the solvent displacement

strategy, hydrogels are initially dispersed in a good solvent (e.g., an organic phase). In this state, the polymer chains are extended and form strong H-bonds with a good solvent, which minimizes the noncovalent interactions between polymer chains. Subsequently, the hydrogels are transferred to a relatively poor solvent solution (e.g., an aqueous phase), where weaker H-bonds are formed, leading to the reformation of intermolecular interactions among the polymers and thus, strengthening of the cross-linked networks for anti-swelling property (Figure 5c).[84,85] Amphiphilic hydrogels containing hydrophobic and hydrophilic moieties can further enhance this effect through hydrophobic associations.[86,87]

Another effective method to create anti-swelling hydrogels is the introduction of thermo-responsive segments.[88] Pluronic F127 (PF127), which consists of poly(ethylene oxide) (PEO) and poly(propylene oxide) (PPO) chains, is a commonly used thermo-responsive amphiphilic polymer for this purpose. PF127 can spontaneously assemble into nanosized micelles,[89] whose PEO core can shrink in a controlled manner upon increasing the temperature above its critical value (Tc). Anti-swelling hydrogels can be developed by introducing PF127 derivatives, such as PF127 diacrylate,[90,91] PF127-bis-(acryloyloxy acetate)[92] (Figure 5d). These thermo-sensitive nano-micellar PF127 derivatives increase the intermolecular strength through thermo-induced shrinkage, thereby enhancing the elastic retractive force and anti-swelling performance of hydrogels.

4.3. Hydrophobized Modifications

Hydrophobic surfaces or architectures are effective in reducing the swelling force of hydrogels by repelling water molecules even when submerged underwater (Figure 5e).[93] This strategy is commonly employed to construct anti-swelling ionogels. Ionic liquids (ILs) or polyionic liquids (PILs) are liquid-like substances with high electrical conductivity that do not readily evaporate. A fully hydrophobic ionogel was proposed through one-step polymerization of hydrophobic acrylate monomers in a hydrophobic IL solvent.[94] The hydrophobic moieties within the polymer network act as diffusion barriers between the ionogel domains and the water phase, reducing the interfacial diffusion of water molecules and ions. Similarly, by polymerizing fluorine-rich IL monomers in a fluorine-rich IL solvent, a hydrophobic ionogel was achieved, exhibiting excellent anti-swelling performance with weight changes of less than 1% in deionized water or seawater over a period of 10 days.[95] Cross-linking a small amount of hydrophobic chains with hydrophilic chains of cross-linkers is also an effective method for anti-swelling hydrogels.[96] This approach not only restricts the movement of molecular chains but also prevents the intrusion of solvent molecules, thereby maintaining the hydrogel's constant size and stability.

5. Anti-Freezing Hydrogels

Hydrogels will lose their intrinsic desirable properties, such as flexibility, toughness, conductivity, and transparency when subjected to freezing at sub-zero temperatures. Therefore, the development of freezing-tolerant hydrogels with reliable performance in low-temperature settings is urgently demanded. The freezing process of water (weakly bonded water) in hydrogels involves a liquid-solid phase transition when the temperature drops below zero at standard atmospheric pressure. This process includes two main steps: i) ice crystal nucleation (in the presence of surface defects, small particles, etc.),[97] ii) ice propagation. The key principle for the design of anti-freezing hydrogels is to inhibit the nucleation and growth process of ice crystals within the hydrogel.

5.1. Ice Nucleation Inhibition

During ice nucleation, the disordered and free water molecules transformed into ordered ice crystal molecules with ordered H-bonds (**Figure 6a**).[98] Disruption of the formation of these ordered H-bonds can lead to ice nucleation inhibition for developing anti-freezing hydrogels. Ice nucleation inhibition mainly includes two strategies: introducing competitive H-bonds and electrostatic interactions. Introducing competitive H-bonds can be performed by introducing organic agents or modification of the polymer chains, during which the newly-formed H-bonds between these introduced substances and water molecules inhibit the nucleation of ice crystals regardless of sub-zero temperature.

Organic agents involving glycerin (GL),[99] ethylene glycol (EG),[100] and dimethyl sulfoxide (DMSO)[101] have been proven to be efficient additives for anti-freezing hydrogels. These organic agents contain abundant functional groups that can form strong H-bonds with water molecules. The stability of these H-bonds is higher than that among water molecules, as depicted in Figure 6b. Some inorganic acids, such as sulfuric acid (H_2SO_4)[102] and phosphoric acid (H_3PO_4),[103] have similar effects. The introduction of water-miscible organic solvents into hydrogels is a straightforward process and can be applied to various hydrogel systems. Additionally, the presence of organic liquids, such as GL, improves the evaporation tolerance of the gels due to their low vapor pressure and high hygroscopicity.[104] However, these additives may escape from the gel network. Therefore, polymer modification has emerged as an effective strategy to "immobilize" the functional groups on the polymer chains of hydrogels (e.g., graft copolymerization). For example, EG can be anchored to polyurethane acrylates via chemical bonds, followed by copolymerization with a PAA matrix. The resulting hydrogel maintained an unfrozen state even at −20 °C.[105] Additionally, hydrogels with more hydrophilic side chains exhibit better anti-freezing performance. This is reasonable since water molecules have a greater tendency to form stronger H-bonds with hydrophilic side chains.[106]

Introducing zwitterions, inorganic salts, ILs, or PILs can also reduce H-bonds among free water molecules in hydrogels (Figure 6c, left). These additives suppress ice nucleation and enable the preparation of freezing-tolerant hydrogels. In our daily lives, inorganic salts are commonly used to prevent snow on roads from freezing. This "water in salt" strategy is based on the strong electrostatic interactions between metal ions and dipolar water molecules. The electrostatic interactions significantly disrupt the internal H-bonds among water molecules, thereby inhibiting ice crystallization. The effect can be approximately calculated by Clausius-Clapeyron equation,[107] namely, $Freezing\ point_{\ total} = Freezing\ point_{water} - \Delta T_f$. Where $\Delta T_f = K_f * m$, m

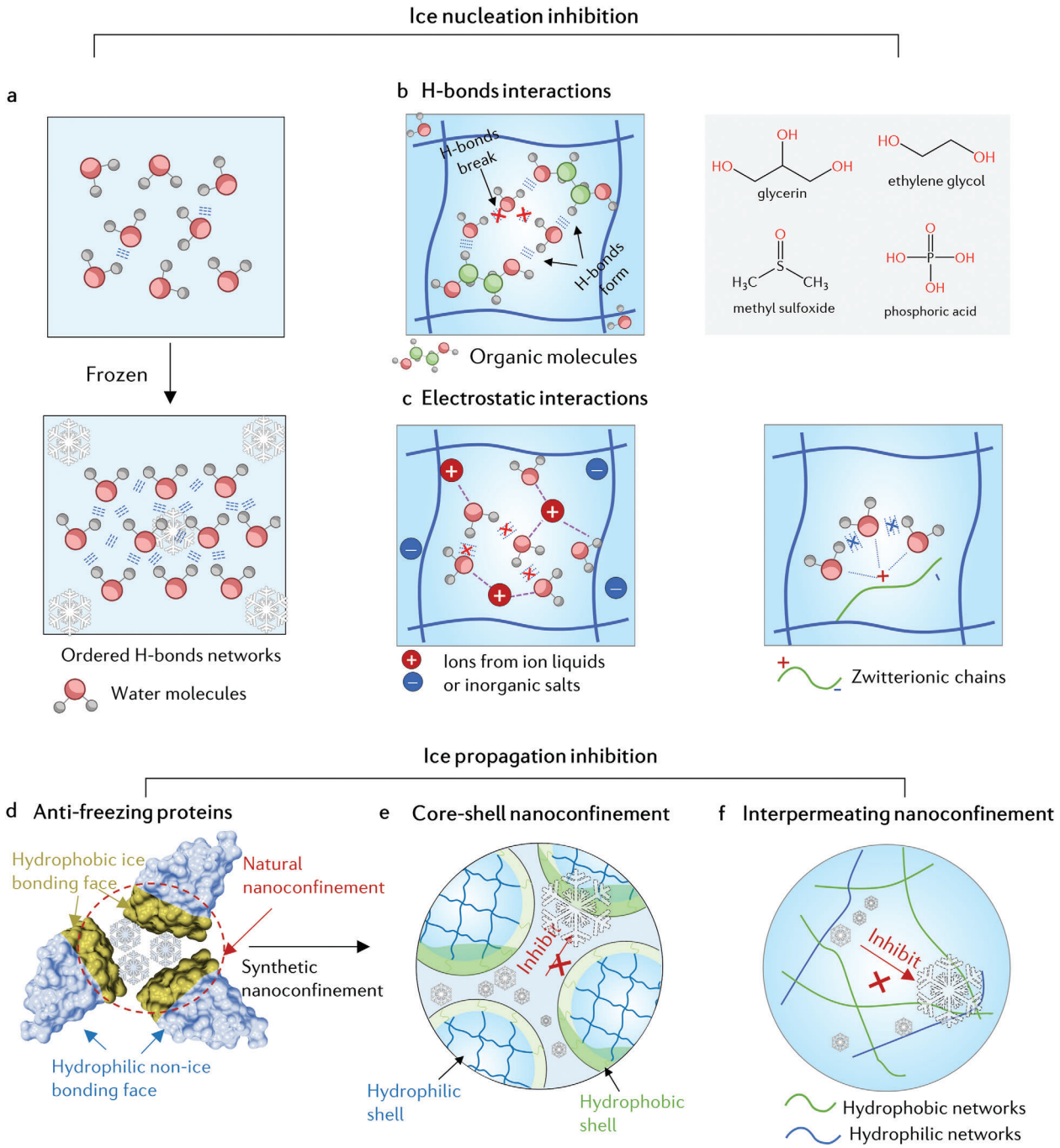

Figure 6. Anti-freezing hydrogels. a) The schematic transformation of disordered and free water molecules into ordered ice crystal molecules. b) Introducing competitive H-bonds for anti-freezing hydrogels. c) Introducing competitive electrostatic interactions for anti-freezing hydrogels. d) Anti-freezing proteins for anti-freezing hydrogels. e) Core-shell nanoconfinement for anti-freezing hydrogels. f) Interpenetrating nanoconfinement for anti-freezing hydrogels.

indicates the molality of the solute and K_f is the cryoscopic constant (1.86 °C kg mol^{-1} for water). This "water in salt" strategy can be extended to design anti-freezing hydrogels. For example, an anti-freezing (−57 °C) PAAm-alginate hydrogel was created by immersing it in different concentrations of $CaCl_2$ solutions, allowing anions and cations to spontaneously diffuse into the hydrogel.[108] ILs[109] (or PILs) can be used to depress the freezing point of hydrogels due to their intrinsic low freezing point and strong electrostatic interactions with water molecules. These anti-freezing ionogels also exhibit low vapor pressure and high ion conductivity, which are widely utilized in flexible electronics over a wide temperature range.[110]

Zwitterionic molecules consist of an ion pair with an equivalent cation and anion, resulting in a neutral overall charge.[111]

Natural zwitterionic materials like proline and betaine can be found in biological organisms, where they play a crucial role in resisting cell damage caused by freezing processes.[112] Taking inspiration from this, zwitterions have been widely employed as additives in anti-freezing hydrogels. The mechanism behind the anti-freezing properties of zwitterions lies in their strong interactions with water molecules through charge-dipole and dipole-dipole interactions (Figure 6c, right).[113] These interactions help retain water in a liquid state even under subzero temperatures. An anti-freezing hydrogel was proposed by incorporating zwitterionic sulfobetaine (SB) and inorganic salts (such as LiCl). By integrating zwitterionic polymer chains derived from SB monomers with a binary solvent system of GL and water, the freezing tolerance (40 °C) of the hydrogel was synergistically enhanced.[103] Additionally, zwitterions not only impart anti-freezing properties to hydrogels but also possess the advantage of anti-FBR, which will be discussed later in this review.

5.2. Ice Propagation Inhibition

Inhibiting the growth of small ice crystals into larger sizes is another significant method for developing anti-freezing materials, including hydrogels. Freezing is difficult to occur in lignified cell walls due to their extremely small size of water-containing microcapillaries (less than 100 nm in diameter) and the strict confinement caused by hydrophobic moieties. As a result, free water in the cell wall tends to supercool rather than crystallize.[114] Taking inspiration from this, ice growth inhibition has been achieved through "soft" nanoconfinement of water molecules.[98] Soft confinement in hydrogels can be achieved by incorporating hydrophobic-hydrophilic moieties from natural anti-freezing proteins, creating confinement such as core/shell nanoconfinement and interpenetrating nanoconfinement.

Many organisms secrete anti-freezing proteins to survive in cold conditions, where ice crystal growth is strictly confined by the hydrophobic ice-binding faces of these proteins (Figure 6d), this nanoconfinement effect leads to the formation of tiny needle-like ice crystals instead of large and sharp ones.[115,116] Some of these anti-freezing proteins have been commercialized and can be directly incorporated into monomer solutions to fabricate anti-freezing hydrogels.[117] Core/shell hydrogel microspheres consist of a hydrophilic core and a hydrophobic shell, where ice crystals are difficult to exist within the hydrophobic shell of each microsphere (Figure 6e). It should be noted that the size of the nano-separation domain must be sufficiently small (e.g., < 4 nm) to form this anti-freezing effect.[118] Interpenetrating nanoconfinement, as the name suggests, is created by interpenetrating hydrophilic and non-hydrophilic moieties (Figure 6f). An interpenetrating organohydrogel was demonstrated by in situ copolymerization of hydrophilic N, N-dimethylacrylamide (DMA), and oleophilic n-butyl methacrylate (BMA).[119] When combined with an organic solvent, these hydrogels with interpenetrating hydrophilic/oleophilic networks significantly reduce the grain size of ice crystals and could even inhibit crystallization altogether even under −78 °C.

In contrast to anti-freezing, high temperatures can also be detrimental to hydrogels, leading to dehydration. Maintaining the water content and stability of hydrogels under high temperature is indeed crucial for their performance in various applications, including electronics and biomedical devices. Strategies to prevent dehydration at high temperatures often overlap with those aimed at anti-freezing hydrogels. This is perhaps because most of the anti-freezing strategies aim to enhance the interactions between free water molecules and additives (organic agents,[120] or inorganic particles,[121] etc.) or modified polymer networks.[122] And these interactions (H-bonds, electrostatic interactions, etc.) also can retain the free water molecules in hydrogels, and thus, prevent dehydration. For instance, in the work by Shi et al., the addition of GL to the mixture of PVA and poly(3,4-)ethylenedioxythiophene doped with polystyrene sulfonate (PEDOT:PSS) facilitated the formation of H-bonds among sulfonic acid groups on PEDOT:PSS, hydroxyl groups on GL, and hydroxyl groups on PVA, thereby improving the thermal stability of the resulting hydrogel fiber. Furthermore, protective coatings on the hydrogel surface serve as a barrier to reduce water loss through evaporation into the surrounding environment. Coatings made from materials like Ecoflex elastomer have been shown to effectively preserve hydrogel integrity for extended periods, minimizing dehydration even under challenging conditions.[123]

6. Anti-FBR Hydrogels

The FBR is a well-known immune-mediated response, during which proteins and cells accumulate around an implanted device, such as implanted hydrogel bioelectronics, resulting in the formation of dense fibroblasts, fibrocytes, and collagenous tissue and the invalidity of the device. Several typical strategies have been developed to achieve anti-FBR hydrogels. These strategies include the use of zwitterions, drug-release surfaces, and modified alginate, among others. Zwitterionic polymers, which contain both positively and negatively charged groups in their repeating units, exhibit an overall neutral charge and form a strong hydration layer through ionic solvation. This cooperative effect makes zwitterionic hydrogels highly resistant to protein and cell adsorption.[111] Various types of zwitterions such as SB,[124] carboxybetaine (CB),[125] phosphorylcholine,[126] have been proposed for anti-FBR hydrogels. These zwitterions-based hydrogels provide superior properties including antifouling, antibacterial, anticoagulant, and immunomodulation during the long-term stage (**Figure 7a**). Peptides or polypeptides derived from amino acids are another type of zwitterionic polymer used in anti-FBR hydrogels.[127] For example, poly-β-homoserine hydrogels can effectively resist fouling from proteins, cells, platelets, and microbes,[128] due to the strong "dual H-bond hydration" generated by the backbone amide bonds and side chain hydroxyl groups. Additionally, various drugs can be employed to combat the FBR.[129] These drugs can be loaded into hydrogels through physical or chemical modifications.[130] Dexamethasone, a typical anti-inflammatory drug, has been widely used in poly(lactic-co-glycolic acid) (PLGA) microsphere/PVA hydrogel coatings to prevent FBR (Figure 7b).[131]

Alginate is a natural, cost-effective, and low-toxicity biomaterial that undergoes mild gelation by adding divalent cations such as Ca^{2+} or Ba^{2+}.[132] However, pristine alginate microspheres still exhibit immunorecognition and induce fibrotic reactions. Therefore, significant efforts have been dedicated to enhancing the

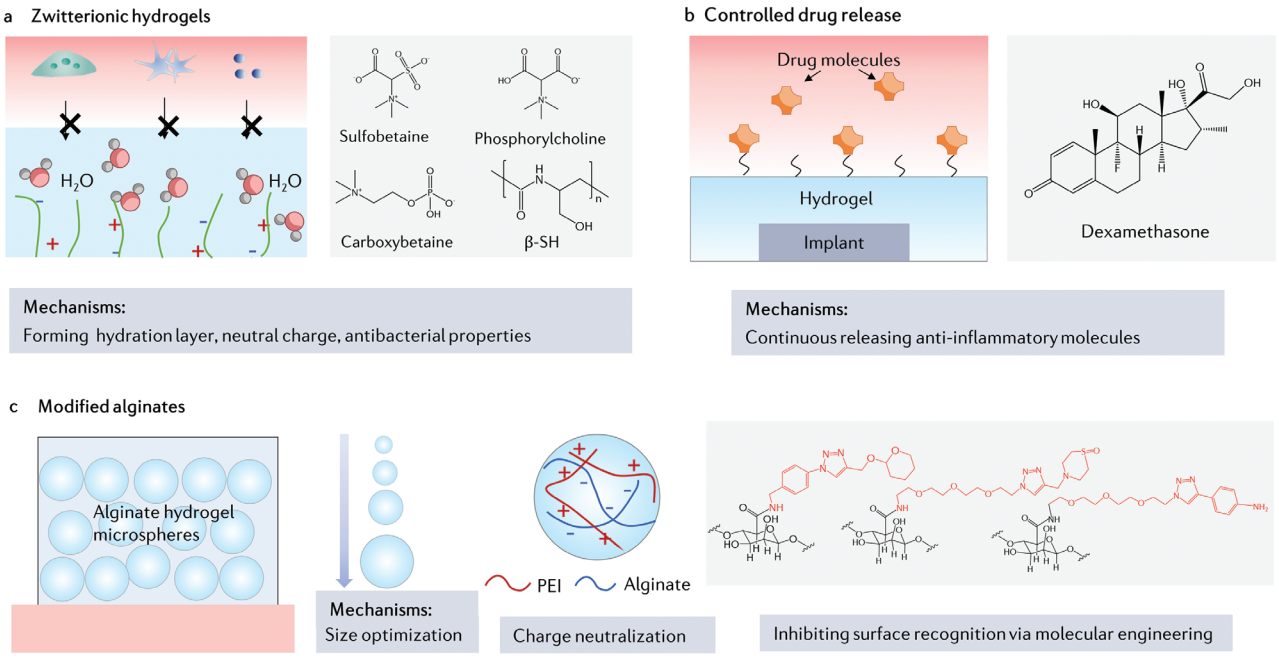

Figure 7. Anti-FBR hydrogels. a) Zwitterionic hydrogels containing a hydration layer and neutral charge to resist FBR. b) Drug-releasing surfaces capable of releasing drugs from the hydrogel surface to suppress FBR at the implant site. c) Rational regulation of size, charge, and chemical composition of alginate hydrogel microspheres for anti-FBR.

anti-FBR of alginate. The size, charge, and chemical composition of alginate play a significant role in its anti-FBR properties (Figure 7c). An interesting study has revealed that alginate microspheres with a diameter of 1.5 mm have the optimal capacity to prevent cellular deposition for at least six months.[133] To address the FBR issue stemming from the negative charge of alginate, a positively charged polyelectrolyte polymer, such as poly (ethylene imine) (PEI) containing protonated ammonium groups, can be combined with alginate. By optimizing the proportion of alginate and PEI, alginate/PEI polyelectrolyte hydrogels with balanced charged and anti-FBR performance have been achieved.[134,135] A combinatorial modification strategy has been employed to synthesize alginate derivatives hydrogel microspheres with various side chains.[136] Among a library of 774 alginate derivatives, three triazole-modified alginate derivatives were carefully selected and proven to effectively resist inflammation and fibrosis when implanted in mice. These lead materials with triazole groups formed a unique hydrogel interface, capable of inhibiting recognition by macrophages and fibrous deposition. However, it should be noted that not all alginate microspheres with triazole structures exhibited anti-inflammatory properties, as other functional groups in these derivatives may also influence the inflammatory response.

7. Bioelectronic Applications

Extreme hydrogels have aroused diverse bioelectronic applications. In this section, we briefly review several examples of extreme hydrogel bioelectronics including hydrogel powering, hydrogel machines, hydrogel wearables, and hydrogel implants. The typical working environments and required extreme properties in each category are discussed.

7.1. Extreme Hydrogel Powering

There is a huge demand for the development of flexible energy storage and supply devices to power portable and wearable electronics. Hydrogels as electrolytes, electrodes, or substrates have become increasingly important in energy devices such as flexible batteries (in particular, zinc-based batteries),[13,137] supercapacitors,[121] and triboelectric nanogenerators (TENG).[138] The temperature has a significant impact on the performance of these energy devices. When hydrogel electrolytes are frozen at subzero temperatures, the mechanical flexibility and ionic conductivity are significantly reduced.[137] Therefore, wide temperature operation is vital for high-performance energy devices. Various anti-freezing strategies have been developed to fabricate temperature-tolerant hydrogel electrolytes for anti-freezing energy devices (**Figure 8a**). These strategies include ice nucleation inhibition by inducing competitive H-bonds,[121] or electrostatic interactions.[139] Introducing ILs is an appealing approach due to their enhanced ionic conductivity, which can simultaneously maintain high electrochemical performance.[139] Adding organic solvents (polyol additives) or inorganic particles is also a commonly adopted anti-freezing strategy. These techniques can enhance not only the low-temperature tolerance but also the high-temperature tolerance (anti-dehydration) of energy devices, widening the upper and lower limits of the working temperature. Chen and his team engineered a borax-crosslinked PVA/glycerol (PVA-B-G) hydrogel. By introducing the competitive H-bonds between glycerol and non-bound water in the hydrogel, the PVA-B-G hydrogels exhibited remarkable anti-freezing performance (could be stretched up to 400%–500% strain low to −35 °C). This unique capability allowed the hydrogel as an effective anti-freezing electrolyte for Zn-MnO_2 batteries.[140] An

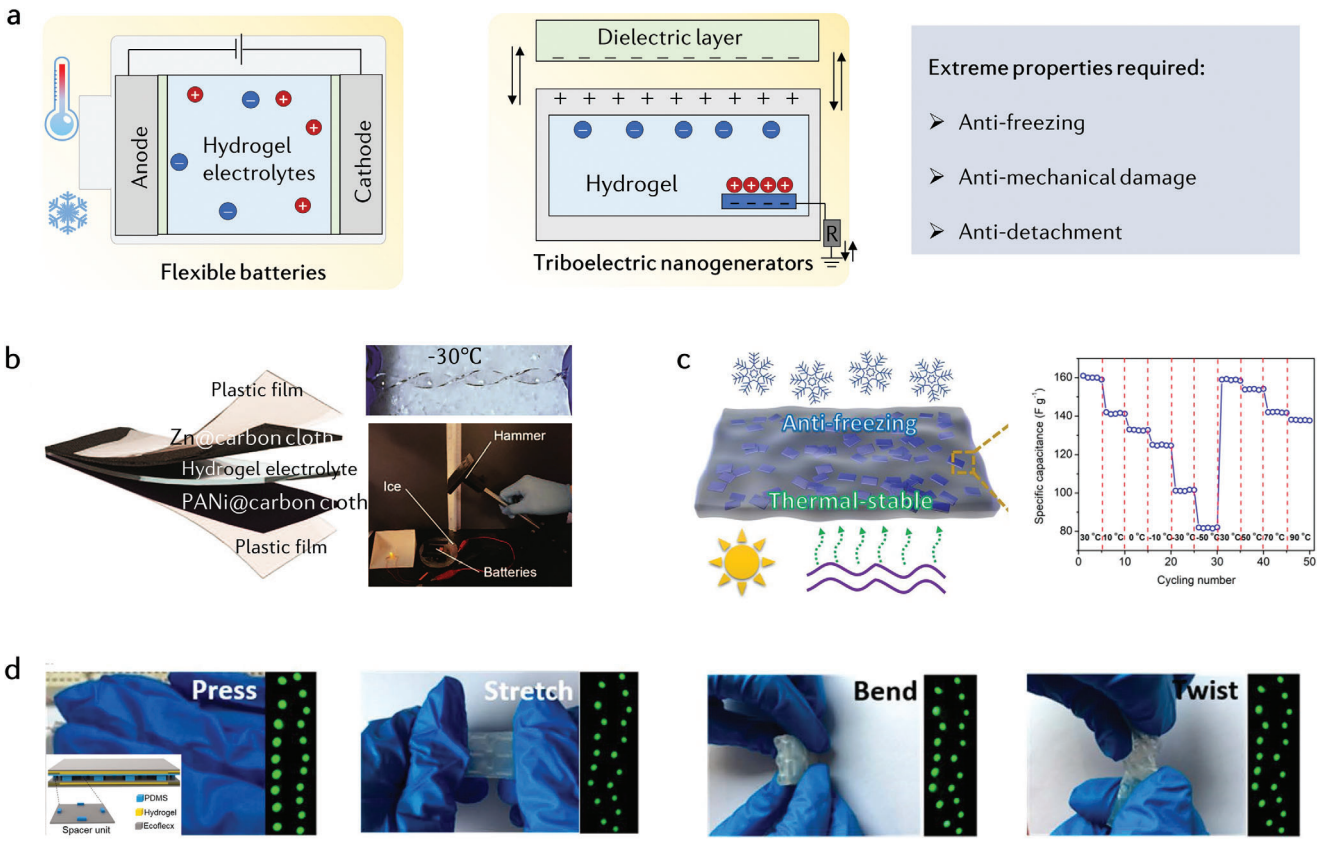

Figure 8. Extreme hydrogel powering. a) The illustration of hydrogel-related energy devices, such as flexible batteries and TENGs, and the required extreme properties. b) An anti-freezing and anti-mechanical damage PVA-based hydrogel electrolyte for zinc-ion batteries. Reproduced with permission.[142] Copyright 2023 John Wiley & Sons. c) A flexible supercapacitor based on an anti-freezing and thermally stable montmorillonite/PVA hydrogel electrolyte. Reproduced with permission.[121] Copyright 2020 American Chemical Society. d) A tough PAAm-alginate hydrogel-based TENG capable of harvesting mechanical energy from pressing, stretching, bending, and twisting motions.[144] Copyright 2018 American Chemical Society.

anti-freezing hydrogel electrolyte based on zinc tetrafluoroborate ($Zn(BF_4)_2$) and PAAm was successfully proposed.[141] The strong interaction between BF_4^- anions and water molecules (O-H-F) in the hydrogel resulted in the disruption of H-bonds among water molecules, effectively inhibiting the formation of ice crystal lattice even at low temperatures. As a demonstration, an anti-freezing and fully integrated flexible $Zn(BF_4)_2$-PAAm-based zinc-ion battery was described, exhibiting high-capacity retention and remarkable cyclic stability even at −70 °C. He's group developed a tough and anti-freezing hydrogel electrolyte for zinc-ion batteries (Figure 8b).[142] On one hand, the introduced inorganic salt (K^+) ions in PVA hydrogels inhibited ice nucleation. On another hand, the open-cell porous structures with strongly aggregated polymer chains provided interpermeating nanoconfinements to prevent ice propagation. Under such a synergistic effect, the freeze-tolerance (< −77 °C), takes a further step toward flexible battery development for harsh environments. In another example, a montmorillonite/PVA hydrogel electrolyte was proposed for flexible supercapacitors with anti-freezing and thermally stable capabilities (Figure 8c).[121] The montmorillonite flakes were added to the PVA hydrogel electrolyte to enhance conductivity. Then, H_2SO_4 and DMSO were introduced to improve anti-freezing as well as anti-dehydration. As a result, the supercapacitor exhibited a wide operation temperature ranging from −50 to 90 °C, with an ionic conductivity of 0.17×10^{-4} S cm^{-1}. Yu et al. designed a PVA, acrylic acid, and H_2SO_4 hydrogel electrolyte (PVA-AA-S) for flexible supercapacitors. The strong interaction between water molecules and PVA chains, as well as PAA chains, prevented the formation of ice crystals.[143] This anti-freezing hydrogel maintained almost 80% of its capacitance after being stored at −35 °C for 23 days.

Beyond anti-freezing performance, hydrogel powering devices need to possess excellent toughness to resist damage and detachment, thereby reducing the occurrence of device damage and potential explosions. Ma et al. designed a sodium polyacrylate (first network)/cellulose (second network) DN hydrogel. The DN design allowed the hydrogel to be stretched to over 1000% strain while maintaining a high ionic conductivity of 0.28 S cm^{-1}.[145] This DN hydrogel electrolyte was successfully integrated into a fiber-like zinc-air battery, demonstrating elongation capabilities of up to 500%. Furthermore, a Zn-MnO_2 battery based on a tough DN hydrogel electrolyte (consisting of PAAm and alginate chains) exhibited stable energy output even under severe mechanical stimuli such as being run over by a car.[146] In the case of hydrogel-based TENGs, a dielectric layer cyclically approaches and moves away from a hydrogel-based electrode. Therefore, superior interfacial linkage (anti-detachment) is crucial to ensure stable and continuous operation during various

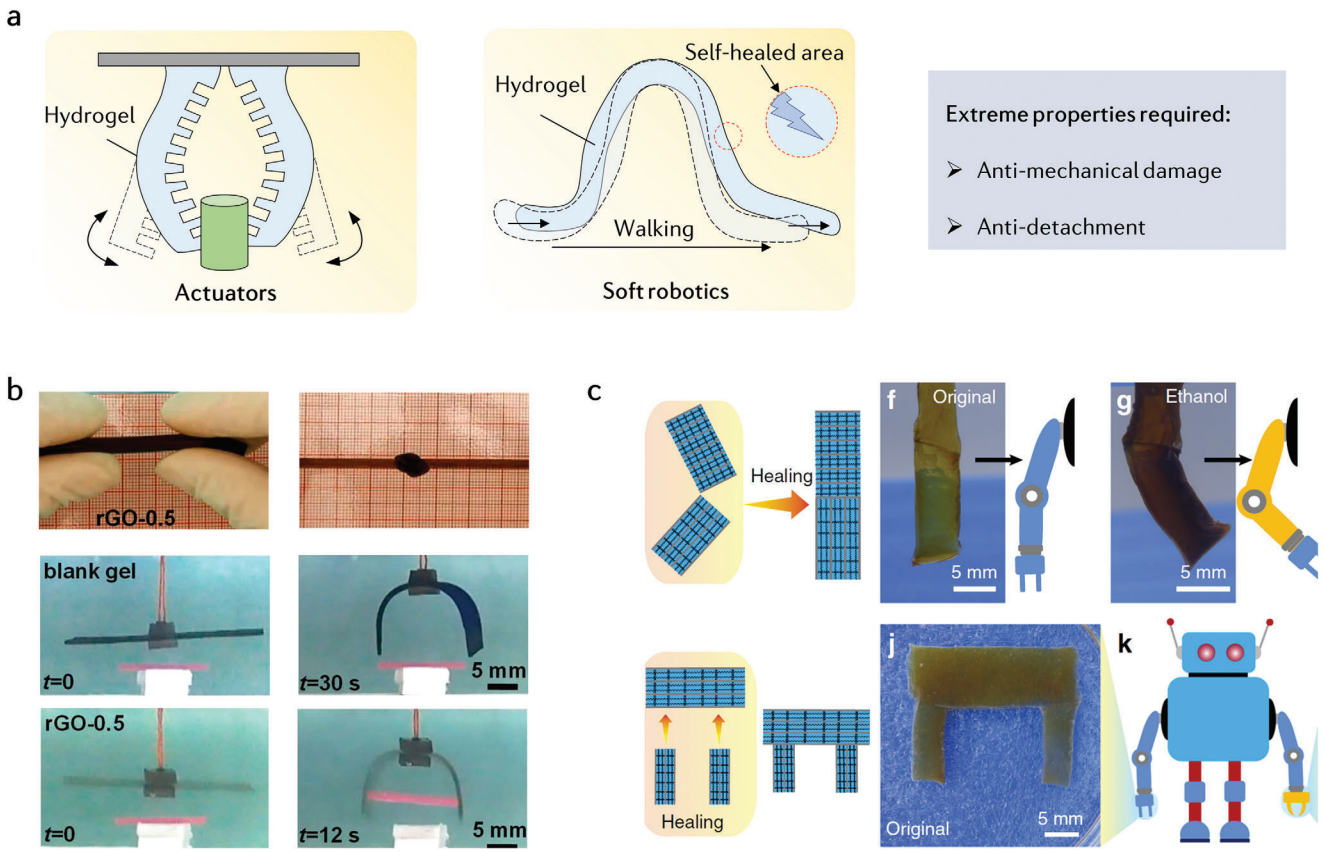

Figure 9. Extreme hydrogel machines. a) The illustration of hydrogel machines, including actuators and soft robotics, and the required extreme properties. b) Comparison of the gripping behaviors of a reference hydrogel and a tough rGO nanocomposite hydrogel. Reproduced with permission.[151] Copyright 2020 American Chemical Society. c) The reconfiguration of A self-healing and reconfigurable robotic based on Ag nanoparticle/PAAm hydrogel. Reproduced with permission.[153] Copyright 2019 Springer Nature.

mechanical motions. Wang's group demonstrated that the use of benzophenone could enhance the bonding between the hydrophilic hydrogel (as the electrode) and the hydrophobic PDMS elastomer (as the electrification layer).[147] This tough hydrogel-based TENG could effectively harvest energy from arbitrary mechanical movements by pressing, stretching, bending, or twisting and illuminating twenty green light-emitting diodes (Figure 8d).[144] Nanocomposite cross-linkers can enhance the stretchability of wearable TENGs for energy harvesting from human motions. For instance, doping MXene nanosheets has been shown to efficiently improve the stretchability of hydrogels, enabling them to be stretched up to 200% of their original length.[148] Additionally, the MXene nanosheets enhanced the conductivity of the hydrogel, resulting in an additional triboelectric output. Consequently, the MXene hydrogel-based TENG achieved an open-circuit voltage measurement of up to 230 V, even in a single-electrode mode.

7.2. Extreme Hydrogel Machines

Hydrogels are highly promising materials for applications in soft robotics and actuators due to their ability to convert external stimuli such as temperature, humidity, pH, electric fields, and light into deformation and movement (**Figure 9a**), due to their inherent flexibility and programmable responsiveness.[149,150] To achieve cyclic loading/unloading, it is crucial to have excellent anti-mechanical damage properties of hydrogel-based machines. In this regard, a tough rGO nanocomposite hydrogel machine was developed using high-functionality cross-links.[151] The presence of -OH and -COOH functional groups on the rGO nanosheets allowed for additional H-bonds interactions with the poly(AMPS-co-AAm) chains. The resulting rGO hydrogel exhibited remarkable tensile strength (≈80 KPa) and compressive strength (1.4 MPa), allowing it to be knotted without damage. Moreover, it could be easily bent to capture a target object within just 12 s under an electric voltage of 30 V (Figure 9b). In comparison, the gel in the control group took 30 s and failed to produce sufficient bending deformation to pick up the target object. In another example, the incorporation of nano-reinforcing domains, such as boron nitride nanosheets, and the use of an organic solvent (GL) simultaneously enhanced the mechanical toughness and low-temperature tolerance of the hydrogel actuators.[104] Zheng et al. fabricated a tough hydrogel actuator through extrusion printing of highly viscous solutions containing P(AA-co-AAm), P(AA-co-NIPAAm), and their mixtures.[152] Gelation occurred immediately when the polymer solutions were transferred into a $FeCl_3$ solution. The gel fibers containing PNIPAm

segments exhibited programmable responsiveness to concentrated saline solutions due to salt-induced collapse and the phase transition of PNIPAm. As a demonstration, a four-armed gripper was designed, which could exert a large output force of up to 115 times the weight of the gripper.

Additionally, it is important to endow self-healing property to hydrogel machines, as they may experience temporary fractures or other damage.[154] In particular, DC network design can be employed to achieve both toughness and self-healing properties, where reversible noncovalent cross-links can effectively dissipate energy during deformation and provide self-healing capabilities.[39] The self-healing property allows for the repair of hydrogel machines, and more importantly, enables the reconfiguration of hydrogel machines by connecting multiple hydrogel pieces together. This opens up possibilities for achieving more complex actuation by combining hydrogel pieces on demand. For example, two or three gel pieces were re-connected to create a solvent-responsive robotic arm/palm based on dynamic reversible covalent bonds (RS-Ag bonds), enabling complex movements like lifting and grasping (Figure 9c).[153] Anti-detachment hydrogels are also necessary for specific functionality in soft machines, such as climbing robots. Huang et al. designed a hydrogel-based climbing robot based on borate ester polymer.[6] The borate ester not only provided self-healing capacity to the hydrogel but also enabled reversible attachment and detachment. By water electrolysis between the hydrogel and the conductive substrate, the interfacial pH could be altered, leading to the reversible cleavage-formation of the borate ester bonds and exposing or shielding the catechol groups. As a result, the hydrogel demonstrated reversible attachment and detachment behavior. Using this controlled adhesive hydrogel as feet and wheels, the tethered walking robots and wheeled robots can climb on both vertical and inverted conductive substrates.

7.3. Extreme Hydrogel Wearables

Hydrogel-based wearable devices have become crucial user-friendly platforms for various applications, such as precision healthcare[155,156] and human-machine interfacing (**Figure 10a**).[157] During the above usage, hydrogel wearables frequently experience various deformations like stretching, compression, and bending. These deformations can induce the formation of microdamage, which may gradually propagate and ultimately lead to material or device failure.[18] The versatile strategies we previously outlined, such as DN, DC, and high-functionality cross-links, offer promising avenues to enhance the mechanical performance of hydrogels, rendering them more compatible with the human body or tissue for wearable bioelectronic applications.

The interpenetrating network design has been widely employed to enhance the stretchability of hydrogel wearables by energy dissipation mechanisms as mentioned earlier. For instance, Wang et al. developed tough conductive hydrogels with interpenetrating networks by in situ oxidation of ANI to PANI network within a P(AAm-co-HEMA) hydrogel matrix (Figure 10b).[158] The reversible H-bonds between the PAAm chains and PANI moieties temporarily ruptured to dissipate energy during loading and rapidly reformed during unloading, thereby improving the toughness of the hydrogel. The PANI/P(AAm-co-HEMA) hydrogel, with the largest toughness of 9.19 MJ m^{-3} achieved after 72 h of oxidation, exhibited an 11-fold increase compared to pristine P(AAm-co-HEMA) hydrogels (0.77 MJ m^{-3}). These hydrogels demonstrated excellent mechanical stability during cyclic tensile and compression loading/unloading tests, which was suitable for long-term and wearable strain-sensing applications. Sani et al. introduced a multifunctional patch containing a hydrogel film for the continuous monitoring and treatment of infected chronic wounds. This patch integrates six distinct sensors to monitor metabolic data from the chronic wound. The flexible, stretchable, and electroactive chondroitin 4-sulfate hydrogel was loaded with drugs. This hydrogel enables electrically controlled delivery of anti-inflammatory and antimicrobial agents to the surrounding area of the wound site.[159]

Hydrogel bioelectronics can still be susceptible to damage when subjected to excessive mechanical stress. To address this challenge, Zhang and colleagues introduced a self-healing hydrogel with the potential for use in wearable organic bioelectronic applications.[160] This hydrogel was composed of a thin layer (1 μm) of the semiconducting polymer PEDOT:PSS. hydrogel exhibited an extremely fast healing response (≈0.1 s) after being wetted with water (Figure 10c). Importantly, the hydrogel also maintained its semiconducting and redox properties after self-healing. This made it an ideal candidate for applications in the field of flexible organic bioelectronics. Hao et al. report a series of multifunctional liquid metal (LM)-hydrogel soft bioelectronics with drug delivery functionality.[161] The hydrogel substrate was achieved by temperature-mediated sol-gel transition of the aqueous mixture of gelatin and alginate with hydrogen and ionic bonding, which were transparent, resilient, healable, and self-adhesive. The gallium-based LM is patterned on the hydrogel substrate through stencil printing, exhibiting high sensitivity to mechanical strain, and capable of detecting tiny motions of a human being. Local iontophoretic drug delivery to specific locations underneath biotissues can also be realized using the LM electrodes.

Flexible wearable bioelectronics typically comprise multiple subsystems, and the bonding of these substructures using adhesive materials such as hydrogels is essential to achieve complete and reliable functionality. Khademhosseini et al. utilized gelatin methacrylate (GelMA) for the development of wearable tactile biosensors, incorporating PEDOT:PSS as transparent electrodes and PDMS/GelMA/PDMS as dielectric layers (Figure 10d).[162] They adopted benzophenone treatment to alleviate of oxygen inhibition effect and made GelMA hydrogels grafted on PDMS by covalent cross-linking under UV light. In this case, an anti-detachment interface between GelMA and PDMS elastomers was constructed. Even after 3000 compression/release cycles (0–0.5 kPa), no significant capacitance reduction or delamination was observed between the GelMA-based core dielectric layer and the PDMS encapsulation layer. This approach ensured the integrity and durability of the wearable system. Bao's group proposed a smart hydrogel-based bandage for on-demand tissue adhesion and detachment.[163] Briefly, they developed PNIPAM hydrogel electrodes that exhibited strong adhesion at room temperature or normal skin temperature but became weakly adhesive (two orders of magnitude lower interfacial energy) when heated above 40 °C (above the lower critical solution temperature). This

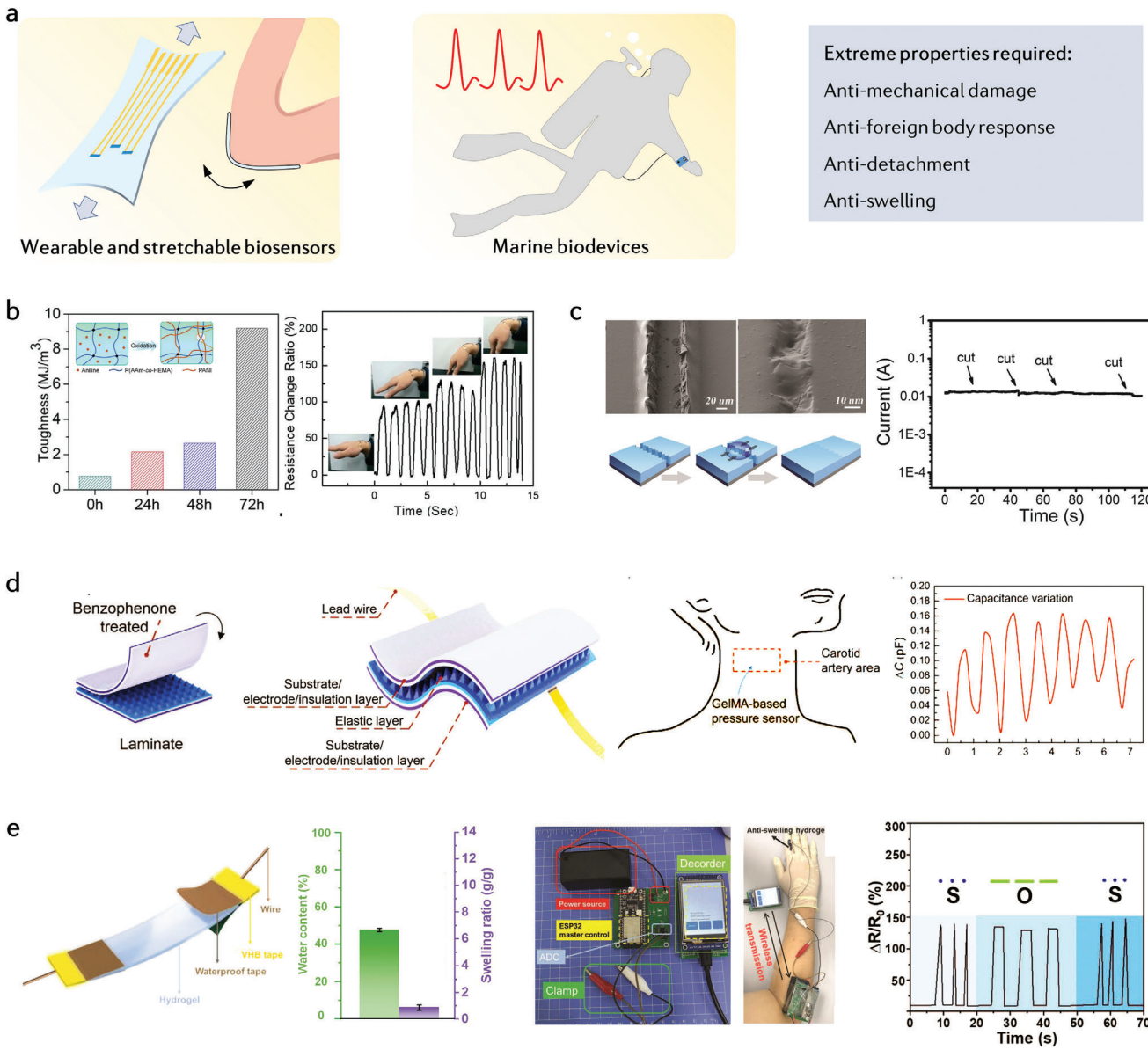

Figure 10. Extreme hydrogel wearables. a) The illustration of hydrogel wearables and the required extreme properties. b) An anti-mechanical damage interpenetrating PANI/P(AAm-co-HEMA) hydrogel for wearable tactile sensing. Reproduced with permission.[158] Copyright 2018 American Chemical Society. c) Electrically self-healing PEDOT:PSS semiconducting hydrogels for wearable bioelectronics. Copyright Reproduced with permission.[160] Copyright 2020 John Wiley & Sons. d) An anti-detachment PDMS/GelMA/PDMS dielectric layer for wearable tactile sensing. Reproduced with permission.[162] Copyright 2020 John Wiley & Sons. e) An underwater electrical device based on an anti-swelling gelatin-PAA-MXene-Zr^{4+} hydrogel. Reproduced with permission.[164] Copyright 2022 John Wiley & Sons.

behavior could be attributed to the aggregated backbones in the PNIPAM hydrogel. The resulting hydrogel with reversible and tunable adhesion could be integrated into a smart bandage with multiple sensors and stimulators for wound monitoring and care.

Underwater wearable sensors based on conductive hydrogels have gained significant interest due to their ability to monitor the movements of divers and ensure their safety. In addition to mechanical toughness, anti-swelling property is desirable for underwater wearable sensors. Anti-swelling conductive hydrogels can be achieved by densification of the cross-link density.[82,165] For example, an anti-swelling PAA/gelatin composite hydrogel was developed using MXene to initiate rapid polymerization of AA, with Zr^{4+} employed to promote gelation (Figure 10e).[164] The dense H-bonds between the gelatin chains of the PAA network and the -NH_2 groups of the gelatin network increased the UCST (upper critical solution temperature) to approximately 31 °C. As a result, the hydrogel exhibited minimal swelling under normal temperature conditions. A wireless underwater communication device was designed using this anti-swelling hydrogel, enabling stable electrical signal output (e.g., Morse codes) by controlling the deformation time of the hydrogel underwater.

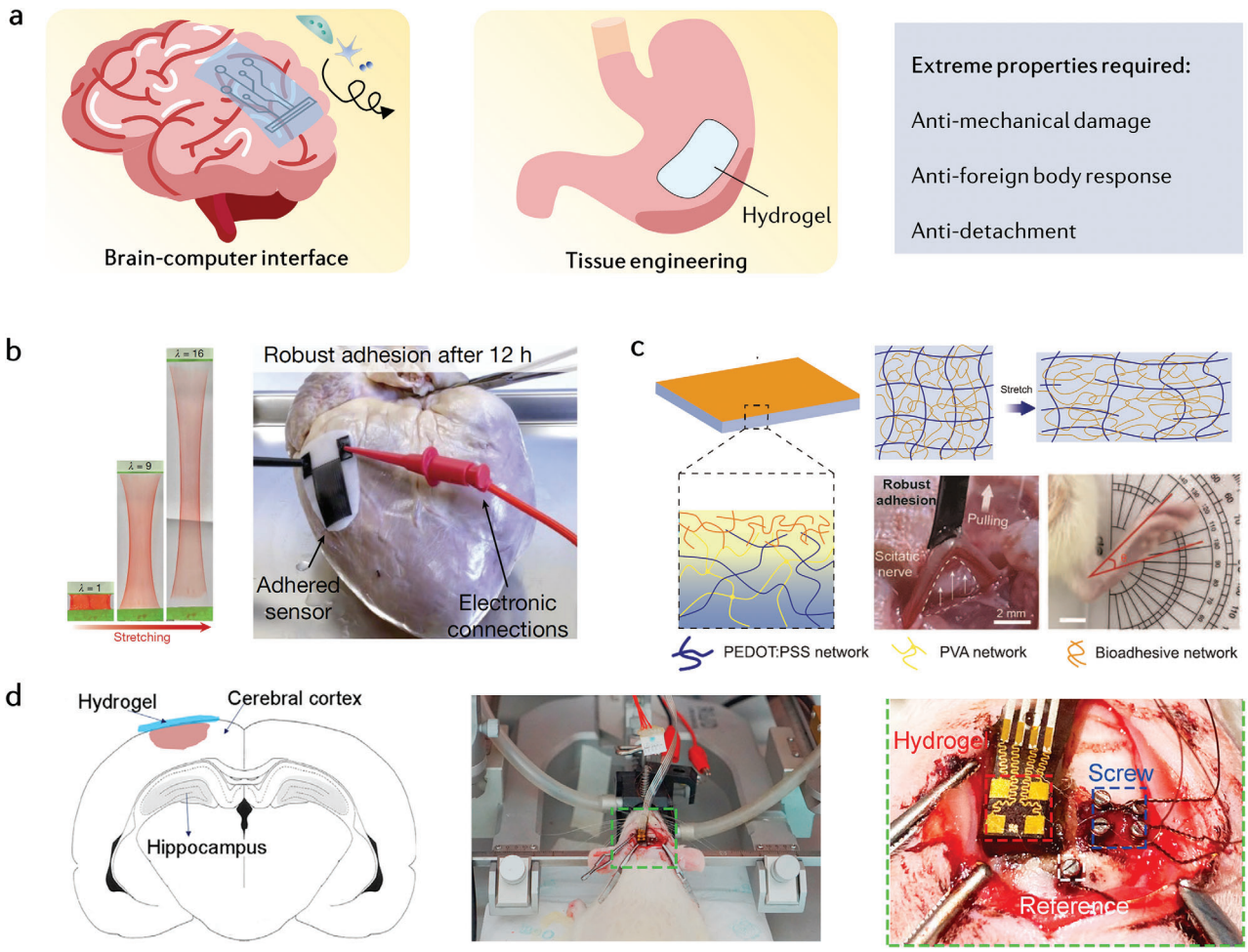

Figure 11. Extreme hydrogel implants. a) The illustration of hydrogel implantable biodevices and the required extreme properties. b) An anti-detachment double-sided hydrogel tape made from DN biopolymers (gelatin or chitosan) and PAA-grafted NHS. Reproduced with permission.[74] Copyright 2019 Springe Nature. c) A highly stretchable and conductive DN PEDOT:PSS-PVA hydrogel with an adhesive layer for implanted neural stimulation. Reproduced with permission.[168] Copyright 2022 John Wiley & Sons. d) An anti-FBR and anti-detachment PDA-PAAm hydrogel for brain-machine interfaces. Reproduced with permission.[25] Copyright 2022 Elsevier.

The anti-swelling property of the hydrogel was crucial for maintaining the stability and functionality of the device. Furthermore, anti-swelling hydrogels with wet adhesion are essential for the design of wearable electrochemical electronics related to epidermal biofluids, such as wound exudate, sweat, and tears. A hydrogel bandage with robust anti-swelling (using PF127 derivatives) and anti-detachment properties (through covalent crosslinks and interlocked microstructures) was employed as a wound dressing.[92] This hydrogel maintained fine adhesion strength in the presence of wound exudate, preventing damage to surrounding nervous tissues due to volume stability (anti-swelling). Wet-adhesive hydrogel patches have also been commonly used for point-of-care testing of sweat in a "just press" manner.[156,166]

7.4. Extreme Hydrogel Implants

In contrast to non-invasive hydrogel wearables that interface with the skin, hydrogel implants are designed to be invasive and introduce foreign materials into the human body (**Figure 11a**). Biocompatibility stands as a paramount requirement in the realm of bioelectronics, especially for implantable applications. Conversely, inadequate compatibility, exemplified by fibrotic encapsulation induced by FBR, can undermine the electrical biosensing and stimulation capacities of implanted electrodes. Such biofouling or FBR poses a significant challenge for implanted hydrogel-based biodevices in the in vivo environment. Anti-FBR hydrogels are urgently needed to reduce the FBR and improve the performance of implanted bioelectronics.[9] Addressing this challenge necessitates the development of anti-FBR hydrogels aimed at mitigating FBR and enhancing the functionality of implanted hydrogel bioelectronics. An anti-FBR implantable glucose biosensor was developed using a hydrogel coating composed of PLGA microspheres dispersed in PVA hydrogels.[130] The PLGA microspheres gradually released drugs at the implantation site to alleviate inflammation and fibrous encapsulation, while the hydrogel facilitated rapid diffusion of analytes to the electrode surface. Liu et al. developed zwitterionic

triazole-poly (TR-SB) hydrogels to reduce FBR and improve blood vessel formation.[167] Compared to conventional alginate hydrogels, the triazole-zwitterionic hydrogel exhibited lower fibrosis and promoted better outcomes in islet encapsulation. It demonstrated diabetes correction for up to approximately one month in mice when implanted in a convenient subcutaneous site. The hydrogel also exhibited high stretchability (250% tensile strain) due to the formation of energy-dissipating π–π stacking through the introduction of triazole moieties into the hydrogel monomers.

The biological adhesion between implanted devices and surrounding tissues/organs is another critical factor to consider. Moisture present on biological tissues poses a challenge to achieving high interfacial toughness. Wet-adhesive hydrogels have been developed for tissue engineering applications, including sealing hemostasis[169] and organ repair.[170] These wet-adhesive interfaces can be combined with other desirable properties of hydrogels, such as anti-mechanical damage, anti-swelling, and anti-FBR. Zhao et al. proposed an anti-detachment and anti-mechanical damage hydrogel tape for bioelectronic applications,[74] which was made from a combination of a biopolymer (gelatin or chitosan) and cross-linked PAA grafted with N-hydrosuccinimide ester (NHS). This hydrogel tape exhibited exceptional toughness, allowing it to stretch to over 16 times its original length because of its DN design. Furthermore, the dry hydrogel tape could absorb interfacial water and undergo in situ cross-linking with the tissue surface. (Figure 11b). As another example, a stretchable strain sensor was attached to a beating porcine heart to measure the deformation of the beating heart. Choi et al. introduced a bioelectronic patch capable of immediate and compliant tissue adhesion, comprising three layers: an ionically conductive tissue adhesive catechol-conjugated alginate hydrogel, a viscoelastic networked film, and a fatigue-resistant conducting composite.[171] The hydrogel layer facilitated conformable tissue adhesion through in situ crosslinking and catechol-based chemical anchorage. This hybrid patch enabled long-term monitoring of electrocardiogram signals in awake rats for up to four weeks of implantation without causing tissue damage. Furthermore, it allowed for spatiotemporal mapping in a myocardial ischemia-reperfusion model. Traditional PEDOT: PSS hydrogel is respectively non-adhesive, rigid, and brittle, which limits its wider application in implantable bioelectronics. To overcome this limitation, Guo et al. first introduced PVA into PEDOT: PSS to construct a DN hydrogel electrode (Figure 11c).[168] The DN PEDOT:PSS/PVA hydrogel exhibited high electrical conductivity (approximately 10 S cm^{-1}) and large stretchability (150%), making it suitable for implanted electromyography recording. Then, a polymeric adhesive layer was added to the surface of the PEDOT: PSS/PVA hydrogel through photopolymerization. This adhesive layer absorbed interfacial water from the tissue and provided robust adhesion (interfacial toughness approximately 600 J m^{-2}) to the tissue through H-bonds. This tough, highly conductive, and adhesive PEDOT:PSS/PVA hydrogel demonstrated high-quality electromyography signal measurement and reliable, low-voltage neural stimulation in a rat model. Recently, a bioadhesive and anti-FBR hydrogel was proposed as an intermediary layer for brain-machine interfaces, which was fabricated by incorporating dopamine methacrylate-hybridized PEDOT nanoparticle into the carrageenan (CA) interpenetrated PDA-polyacrylamide (CA-PDA-PAM) network hydrogel (Figure 11d).[25] The catechol groups in the hydrogel formed various non-covalent and covalent bonds with the underlying brain tissue, achieving robust adhesion between rigid metallic electronic microcircuits and soft brain tissue. Additionally, the catechol groups minimized inflammation and fibrosis, reducing neuroinflammation and limiting glial and astrocyte activation by regulating macrophage activity. This bioadhesive and anti-FBR hydrogel allowed long-term and accurate electroencephalographic signal monitoring.

8. Summary and Outlook

The past several decades have witnessed the rise of extreme hydrogel bioelectronics. Compared with traditional hydrogels, extreme hydrogels mitigate structure and function loss when exposed to harsh conditions, essential for hydrogel powering, machines, wearables and implants, etc. Although tremendous efforts made, challenges and opportunities still exist.

1) First, quantitative standards should be established to define the extreme functionalities. For example, it is easily understandable that anti-freezing hydrogel electronics refer to the hydrogels that can maintain unfrozen statues lower than 0 °C under standard atmospheric pressure. Anti-swelling hydrogels are usually termed as having a low swelling ratio, however, there is no strictly quantitative standard for the swelling ratio. A similar situation can be found in anti-detachment anti-FBR hydrogels, etc. A well-defined standard will help benchmark the basic properties of those extreme hydrogels.
2) Second, advanced characterization techniques are urgently needed. The current understanding of the interactions between polymer chains and water molecules, organic molecules, and micro/nanocomposites is still in the early stages. Several tools, such as high-throughput screening and in situ scope techniques can help us visualize various chemical and physical interactions and unveil the structure-property relationships during the design and fabrication process of extreme hydrogel. Only in this way on-demand regulation and prediction of the hydrogels' properties under extreme conditions is possible. Besides, operando characterizations of multiple parameters of hydrogels in various specific conditions are essential to gain deeper insight into material properties.
3) Third, the modification strategies for extreme hydrogel bioelectronics must be performed moderately. Some strategies rely on introducing external substances (e.g., electronic elements) to the pristine hydrogels. However, the impact of the foreign substances on the intrinsic performances of hydrogels should be carefully evaluated for compromise. For example, nanocomposites are conducive to constructing tough hydrogels with high conductivity, nevertheless, excessive nanocomposites will result in a low water content or low elongation at break of hydrogels.[172] Attention should be paid to how to address these dilemmas.
4) Fourth, achieving multiple extreme functionalities into one hydrogel will bring new values. While the single extreme property of hydrogel has been extensively investigated, the practical working environments may be more complex, which require multiple extreme properties. For example, anti-freezing hydrogel bioelectronics with anti-detachment

properties are appealing in subzero environments, which are relatively less explored. Integrated anti-FBR and anti-swelling hydrogels will greatly accelerate the development and clinical application of implantable biodevices.

5) Fifth, new extreme properties need to be further explored. For example, there is an urgent need to develop anti-salinity hydrogel electronics for applications in deep-sea environments. Additionally, an anti-CO_2 hydrogel electrolyte is necessary for alkaline zinc-based batteries to work under a high CO_2 concentration condition.[13]

Overall, extreme hydrogel bioelectronics is a highly interdisciplinary area, which requires close cooperation between researchers and engineers from different fields. For example, material scientists developing hydrogels should gain feedback from biomedical researchers to tailor material properties for practical use. Besides, convergent engineering among experts in materials, devices, and systems is a must to advance extreme hydrogel bioelectronics for various applications in real-world scenarios.

Acknowledgements

S.Z. acknowledges grants from the Collaborative Research Fund (C7005-23Y) from the Research Grants Council of the Hong Kong SAR Government, the Innovation and Technology Fund (Mainland-Hong Kong Joint Funding Scheme, MHP/053/21) of the Hong Kong SAR Government, the Shenzhen-Hong Kong-Macau Technology Research Programme (SGDX20210823103537034), and the Seed Funding for Strategic Interdisciplinary Research Scheme from the University of Hong Kong. T.X. acknowledges grants from Shenzhen University 2035 Pursuit of Excellence Research Program (8690100000221) and Joint Fund of the Ministry of Education for Equipment Preresearch (8091B022142). [Correction added on June 24, 2024, after first online publication: Typographical errors have been updated in this version.]

Conflict of Interest

The authors declare no conflict of interest.

Keywords

bioelectronics, biological interfaces, extreme conditions, hydrogels, wearables and implants

Received: April 7, 2024
Revised: May 14, 2024
Published online: June 20, 2024

[1] S. Gong, Y. Lu, J. Yin, A. Levin, W. Cheng, *Chem. Rev.* **2024**, *124*, 455.
[2] R. Liu, Z. L. Wang, K. Fukuda, T. Someya, *Nat. Rev. Mater.* **2022**, *7*, 870.
[3] O. Wichterle, D. LÍM, *Nature* **1960**, *185*, 117.
[4] Y. S. Zhang, A. Khademhosseini, *Science* **2017**, 356,
[5] C. Yang, Z. Suo, *Nat. Rev. Mater.* **2018**, *3*, 125.
[6] J. Huang, Y. Liu, Y. Yang, Z. Zhou, J. Mao, T. Wu, J. Liu, Q. Cai, C. Peng, Y. Xu, B. Zeng, W. Luo, G. Chen, C. Yuan, L. Dai, *Sci. Robot.* **2021**, *6*, eabe1858.
[7] X. Q. Wang, K. H. Chan, W. Lu, T. Ding, S. W. L. Ng, Y. Cheng, T. Li, M. Hong, B. C. K. Tee, G. W. Ho, *Nat. Commun.* **2022**, *13*, 3369.
[8] Y. Zhao, C. Xuan, X. Qian, Y. Alsaid, M. Hua, L. Jin, X. He, *Sci. Robot.* **2019**, *4*, eaax7112.
[9] H. Yuk, J. Wu, X. Zhao, *Nat. Rev. Mater.* **2022**, *7*, 935.
[10] H. Yuk, B. Lu, X. Zhao, *Chem. Soc. Rev.* **2019**, *48*, 1642.
[11] T. Zhu, Y. Ni, G. M. Biesold, Y. Cheng, M. Ge, H. Li, J. Huang, Z. Lin, Y. Lai, *Chem. Soc. Rev.* **2023**, *52*, 473.
[12] J. Tan, B. Kang, K. Kim, D. Kang, H. Lee, S. Ma, G. Jang, H. Lee, J. Moon, *Nat. Energy* **2022**, *7*, 537.
[13] S. Zhao, Y. Zuo, T. Liu, S. Zhai, Y. Dai, Z. Guo, Y. Wang, Q. He, L. Xia, C. Zhi, J. Bae, K. Wang, M. Ni, *Adv. Energy Mater.* **2021**, *11*, 2101749.
[14] Z. Wu, Q. Ding, H. Wang, J. Ye, Y. Luo, J. Yu, R. Zhan, H. Zhang, K. Tao, C. Liu, J. Wu, *Adv. Funct. Mater.* **2023**, *34*, 2308280.
[15] D. Wang, D. Zhang, M. Tang, H. Zhang, T. Sun, C. Yang, R. Mao, K. Li, J. Wang, *Nat. Energy* **2022**, *100*, 107509.
[16] S. Jin, H. Choi, D. Seong, C.-L. You, J.-S. Kang, S. Rho, W. B. Lee, D. Son, M. Shin, *Nature* **2023**, *623*, 58.
[17] F. Wang, Y. Xue, X. Chen, P. Zhang, L. Shan, Q. Duan, J. Xing, Y. Lan, B. Lu, J. Liu, *Adv. Funct. Mater.* **2023**, 2314471.
[18] Z. Bao, C. Xian, Q. Yuan, G. Liu, J. Wu, *Adv. Healthcare Mater.* **2019**, *8*, 1900670.
[19] E. Dondossola, P. Friedl, *Nat. Rev. Mater.* **2021**, *7*, 6.
[20] D. W. Grainger, *Nat. Biotechnol.* **2013**, *31*, 507.
[21] T. Zhou, H. Yuk, F. Hu, J. Wu, F. Tian, H. Roh, Z. Shen, G. Gu, J. Xu, B. Lu, X. Zhao, *Nat. Mater.* **2023**, *22*, 895.
[22] J. Deng, H. Yuk, J. Wu, C. E. Varela, X. Chen, E. T. Roche, C. F. Guo, X. Zhao, *Nat. Mater.* **2021**, *20*, 229.
[23] S. He, X. Sun, Z. Qin, X. Dong, H. Zhang, M. Shi, F. Yao, H. Zhang, J. Li, *Adv. Mater. Technol.* **2021**, *7*, 2101343.
[24] D. Jiang, H. Wang, S. Wu, X. Sun, J. Li, *Small Methods* **2022**, *6*, 2101043.
[25] X. Wang, X. Sun, D. Gan, M. Soubrier, H.-Y. Chiang, L. Yan, Y. Li, J. Li, S. Yu, Y. Xia, K. Wang, Q. Qin, X. Jiang, L. Han, T. Pan, C. Xie, X. Lu, *Matter* **2022**, *5*, 1204.
[26] S. Naficy, H. R. Brown, J. M. Razal, G. M. Spinks, P. G. Whitten, *Aust. J. Chem.* **2011**, *64*, 1007.
[27] J. P. Gong, Y. Katsuyama, T. Kurokawa, Y. Osada, *Adv. Mater.* **2003**, *15*, 1155.
[28] R. E. Webber, C. Creton, H. R. Brown, J. P. Gong, *Macromolecules* **2007**, *40*, 2919.
[29] H. Zhang, X. Gan, Z. Song, J. Zhou, *Angew. Chem., Int. Ed.* **2023**, *62*, 202217833.
[30] Y. Yang, X. Wang, F. Yang, H. Shen, D. Wu, *Adv. Mater.* **2016**, *28*, 7178.
[31] Z. Tao, H. Fan, J. Huang, T. Sun, T. Kurokawa, J. P. Gong, *ACS Appl. Mater. Interfaces* **2019**, *11*, 37139.
[32] J. Y. Sun, X. Zhao, W. R. Illeperuma, O. Chaudhuri, K. H. Oh, D. J. Mooney, J. J. Vlassak, Z. Suo, *Nature* **2012**, *489*, 133.
[33] B. Zhang, Z. Gao, G. Gao, W. Zhao, J. Li, X. Ren, *Macromol. Mater. Eng.* **2018**, *303*, 1800072.
[34] H. J. Zhang, T. L. Sun, A. K. Zhang, Y. Ikura, T. Nakajima, T. Nonoyama, T. Kurokawa, O. Ito, H. Ishitobi, J. P. Gong, *Adv. Mater.* **2016**, *28*, 4884.
[35] X. Li, C. Tang, D. Liu, Z. Yuan, H. C. Hung, S. Luozhong, W. Gu, K. Wu, S. Jiang, *Adv. Mater.* **2021**, *33*, 2102479.
[36] T. Matsuda, R. Kawakami, R. Namba, T. Nakajima, J. P. Gong, *Science* **2019**, *363*, 504.
[37] H. Lei, L. Dong, Y. Li, J. Zhang, H. Chen, J. Wu, Y. Zhang, Q. Fan, B. Xue, M. Qin, B. Chen, Y. Cao, W. Wang, *Nat. Commun.* **2020**, *11*, 4032.
[38] Z. Li, X. Meng, W. Xu, S. Zhang, J. Ouyang, Z. Zhang, Y. Liu, Y. Niu, S. Ma, Z. Xue, A. Song, S. Zhang, C. Ren, *Soft Matter* **2020**, *16*, 7323.

[39] Z. Jiang, B. Diggle, I. C. G. Shackleford, L. A. Connal, *Adv. Mater.* **2019**, *31*, 1904956.
[40] T. Liu, Z. Xie, M. Chen, S. Tang, Y. Liu, J. Wang, R. Zhang, H. Wang, X. Guo, A. Gu, Y. Yuan, N. Wang, *Chem. Eng. J.* **2022**, *430*, 133182.
[41] S. Lin, X. Liu, J. Liu, H. Yuk, H. C. Loh, G. A. Parada, C. Settens, J. Song, A. Masic, G. H. McKinley, X. Zhao, *Sci. Adv.* **2019**, *5*, eaau8528.
[42] J. Liu, S. Lin, X. Liu, Z. Qin, Y. Yang, J. Zang, X. Zhao, *Nat. Commun.* **2020**, *11*, 1071.
[43] T. Huang, H. G. Xu, K. X. Jiao, L. P. Zhu, H. R. Brown, H. L. Wang, *Adv. Mater.* **2007**, *19*, 1622.
[44] S. Liu, X. Wang, Y. Peng, Z. Wang, R. Ran, *Macromol. Mater. Eng.* **2021**, *306*, 2100198.
[45] T. Xu, H. Du, H. Liu, W. Liu, X. Zhang, C. Si, P. Liu, K. Zhang, *Adv. Mater.* **2021**, *33*, 2101368.
[46] A. K. Gaharwar, N. A. Peppas, A. Khademhosseini, *Biotechnol. Bioeng.* **2014**, *111*, 441.
[47] K. Haraguchi, T. Takehisa, *Adv. Mater.* **2002**, *14*, 1120.
[48] S. Rose, A. Dizeux, T. Narita, D. Hourdet, A. Marcellan, *Macromolecules* **2013**, *46*, 4095.
[49] L. Han, X. Lu, M. Wang, D. Gan, W. Deng, K. Wang, L. Fang, K. Liu, C. W. Chan, Y. Tang, L.-T. Weng, H. Yuan, *Small* **2016**, *13*, 1601916.
[50] T. Sakai, T. Matsunaga, Y. Yamamoto, C. Ito, R. Yoshida, S. Suzuki, N. Sasaki, M. Shibayama, U. Chung, *Macromolecules* **2008**, *41*, 5379.
[51] Y. Okumura, K. Ito, *Adv. Mater.* **2001**, *13*, 485.
[52] P. Ghaderinejad, N. Najmoddin, Z. Bagher, M. Saeed, S. Karimi, S. Simorgh, M. Pezeshki-Modaress, *Chem. Eng. J.* **2021**, *420*, 130465.
[53] M. Hua, S. Wu, Y. Ma, Y. Zhao, Z. Chen, I. Frenkel, J. Strzalka, H. Zhou, X. Zhu, X. He, *Nature* **2021**, *590*, 594.
[54] D. L. Taylor, *Adv. Mater.* **2016**, *28*, 9060.
[55] Y. Liu, S. H. Hsu, *Front. Chem.* **2018**, *6*, 449.
[56] A. Zhang, Y. Liu, D. Qin, M. Sun, T. Wang, X. Chen, *Int. J. Biol. Macromol.* **2020**, *164*, 2108.
[57] W. Yang, B. Shao, T. Liu, Y. Zhang, R. Huang, F. Chen, Q. Fu, *ACS Appl. Mater. Interfaces* **2018**, *10*, 8245.
[58] S. Hong, T. Park, J. Lee, Y. Ji, J. Walsh, T. Yu, J. Y. Park, J. Lim, C. B. Alston, L. Solorio, H. Lee, Y. L. Kim, D. R. Kim, C. H. Lee, *ACS Sens.* **2024**, *9*, 662.
[59] S. Dai, X. Zhou, S. Wang, J. Ding, N. Yuan, *Nanoscale* **2018**, *10*, 19360.
[60] T. Zhang, H. Yuk, S. Lin, G. A. Parada, X. Zhao, *Acta Mech. Sinica-PRC* **2017**, *33*, 543.
[61] H. Fan, J. Wang, Z. Jin, *Macromolecules* **2018**, *51*, 1696.
[62] H. Fan, J. Wang, Z. Tao, J. Huang, P. Rao, T. Kurokawa, J. P. Gong, *Nat. Commun.* **2019**, *10*, 5127.
[63] J. Saiz-Poseu, J. Mancebo-Aracil, F. Nador, F. Busque, D. Ruiz-Molina, *Angew. Chem., Int. Ed.* **2019**, *58*, 696.
[64] H. Yuk, T. Zhang, S. Lin, G. A. Parada, X. Zhao, *Nat. Mater.* **2016**, *15*, 190.
[65] X. Yao, J. Liu, C. Yang, X. Yang, J. Wei, Y. Xia, X. Gong, Z. Suo, *Adv. Mater.* **2019**, *31*, 1903062.
[66] J. Yang, R. Bai, Z. Suo, *Adv. Mater.* **2018**, *30*, 1800671.
[67] Z. Ma, C. Bourquard, Q. Gao, S. Jiang, T. De Iure-Grimmel, R. Huo, X. Li, Z. He, Z. Yang, G. Yang, Y. Wang, E. Lam, Z. H. Gao, O. Supponen, J. Li, *Science* **2022**, *377*, 751.
[68] S. Ji, X. Chen, *Nat. Sci. Rev.* **2023**, *10*, nwac172.
[69] S. Y. Yang, E. D. O'Cearbhaill, G. C. Sisk, K. M. Park, W. K. Cho, M. Villiger, B. E. Bouma, B. Pomahac, J. M. Karp, *Nat. Commun.* **2013**, *4*, 1702.
[70] D. Gan, W. Xing, L. Jiang, J. Fang, C. Zhao, F. Ren, L. Fang, K. Wang, X. Lu, *Nat. Commun.* **2019**, *10*, 1487.
[71] F. Pan, S. Ye, R. Wang, W. She, J. Liu, Z. M. Sun, W. Zhang, *Mater. Horiz.* **2020**, *7*, 2063.
[72] Y. Zhou, C. Zhang, S. Gao, B. Zhang, J. Sun, J.-j. Kai, B. Wang, Z. Wang, *Chem. Mater.* **2021**, *33*, 8822.
[73] Z. Wang, L. Guo, H. Xiao, H. Cong, S. Wang, *Mater. Horiz.* **2020**, *7*, 282.
[74] H. Yuk, C. E. Varela, C. S. Nabzdyk, X. Mao, R. F. Padera, E. T. Roche, X. Zhao, *Nature* **2019**, *575*, 169.
[75] X. Peng, X. Xia, X. Xu, X. Yang, B. Yang, P. Zhao, W. Yuan, P. W. Y. Chiu, L. Bian, *Sci. Adv.* **2021**, *7*, abe8739.
[76] J. Deng, H. Yuk, J. Wu, C. E. Varela, X. Chen, E. T. Roche, C. F. Guo, X. Zhao, *Nat. Mater.* **2020**, *20*, 229.
[77] P. Rao, T. L. Sun, L. Chen, R. Takahashi, G. Shinohara, H. Guo, D. R. King, T. Kurokawa, J. P. Gong, *Adv. Mater.* **2018**, *30*, 1801884.
[78] B. Zhang, L. Jia, J. Jiang, S. Wu, T. Xiang, S. Zhou, *ACS Appl. Mater. Interfaces* **2021**, *13*, 36574.
[79] Y. Zhan, W. Fu, Y. Xing, X. Ma, C. Chen, *Mater. Sci. Eng. C* **2021**, *127*, 112208.
[80] X. Li, H. Wang, D. Li, S. Long, G. Zhang, Z. Wu, *ACS Appl. Mater. Interfaces* **2018**, *10*, 31198.
[81] J. Wu, Z. Pan, Z. Y. Zhao, M. H. Wang, L. Dong, H. L. Gao, C. Y. Liu, P. Zhou, L. Chen, C. J. Shi, Z. Y. Zhang, C. Yang, S. H. Yu, D. H. Zou, *Adv. Mater.* **2022**, *34*, 2200115.
[82] C. Qi, Z. Dong, Y. Huang, J. Xu, C. Lei, *ACS Appl. Mater. Interfaces* **2022**, *14*, 30385.
[83] X. Luo, M. Y. Akram, Y. Yuan, J. Nie, X. Zhu, *J. Appl. Polym. Sci.* **2019**, *136*, 46895.
[84] L. Xu, S. Gao, Q. Guo, C. Wang, Y. Qiao, D. Qiu, *Adv. Mater.* **2020**, *32*, 2004579.
[85] X. Liu, Q. Zhang, L. Duan, G. Gao, *ACS Appl. Mater. Interfaces* **2019**, *11*, 6644.
[86] Q. Feng, K. Wei, K. Zhang, B. Yang, F. Tian, G. Wang, L. Bian, *NPG Asia Mater.* **2018**, *10*, e455.
[87] X. Liu, Q. Zhang, G. Gao, *ACS Nano* **2020**, *14*, 13709.
[88] H. Kamata, Y. Akagi, Y. Kayasuga-Kariya, U. I. Chung, T. Sakai, *Science* **2014**, *343*, 873.
[89] M. S. Akash, K. Rehman, *J. Control Rel.* **2015**, *209*, 120.
[90] P. Ren, H. Zhang, Z. Dai, F. Ren, Y. Wu, R. Hou, Y. Zhu, J. Fu, *J. Mater. Chem. B* **2019**, *7*, 5490.
[91] C. Shen, Y. Li, Y. Wang, Q. Meng, *Lab Chip* **2019**, *19*, 3962.
[92] S. Bian, L. Hao, X. Qiu, J. Wu, H. Chang, G.-M. Kuang, S. Zhang, X. Hu, Y. Dai, Z. Zhou, F. Huang, C. Liu, X. Zou, W. Liu, W. W. Lu, H. Pan, X. Zhao, *Adv. Funct. Mater.* **2022**, *32*, 2207741.
[93] X. Yao, L. Chen, J. Ju, C. Li, Y. Tian, L. Jiang, M. Liu, *Adv. Mater.* **2016**, *28*, 7383.
[94] J. Wei, Y. Zheng, T. Chen, *Mater. Horiz.* **2021**, *8*, 2761.
[95] Z. Yu, P. Wu, *Adv. Mater.* **2021**, *33*, 2008479.
[96] H. An, M. Zhang, Z. Huang, Y. Xu, S. Ji, Z. Gu, P. Zhang, Y. Wen, *Adv. Mater.* **2023**, *36*, 2310164.
[97] H. Desnos, A. Baudot, M. Teixeira, G. Louis, L. Commin, S. Buff, P. Bruyère, *Thermochim. Acta* **2018**, *667*, 193.
[98] Y. Xu, Q. Rong, T. Zhao, M. Liu, *Giant* **2020**, *2*, 100014.
[99] W. Shi, Z. Wang, H. Song, Y. Chang, W. Hou, Y. Li, G. Han, *ACS Appl. Mater. Interfaces* **2022**, *14*, 35114.
[100] Q. Rong, W. Lei, L. Chen, Y. Yin, J. Zhou, M. Liu, *Angew. Chem. Int. Ed.* **2017**, *56*, 14159.
[101] D. B. Wong, K. P. Sokolowsky, M. I. El-Barghouthi, E. E. Fenn, C. H. Giammanco, A. L. Sturlaugson, M. D. Fayer, *J. Phys. Chem. B* **2012**, *116*, 5479.
[102] B. Yao, S. Wu, R. Wang, Y. Yan, A. Cardenas, D. Wu, Y. Alsaid, W. Wu, X. Zhu, X. He, *Adv. Funct. Mater.* **2021**, *32*, 2109506.
[103] J. Xu, R. Jin, X. Ren, G. Gao, *Chem. Eng. J.* **2021**, *413*, 127446.
[104] M. Guo, Y. Wu, S. Xue, Y. Xia, X. Yang, Y. Dzenis, Z. Li, W. Lei, A. T. Smith, L. Sun, *J. Mater. Chem. A* **2019**, *7*, 25969.
[105] F. Mo, G. Liang, Q. Meng, Z. Liu, H. Li, J. Fan, C. Zhi, *Energ. Environ. Sci.* **2019**, *12*, 706.
[106] Y. Jian, S. Handschuh-Wang, J. Zhang, W. Lu, X. Zhou, T. Chen, *Matter. Horiz.* **2021**, *8*, 351.

[107] O. L. I. Brown, *J. Chem. Educ.* **1951**, *28*, 428.
[108] X. P. Morelle, W. R. Illeperuma, K. Tian, R. Bai, Z. Suo, J. J. Vlassak, *Adv. Mater.* **2018**, *30*, 1801541.
[109] Y. Ding, J. Zhang, L. Chang, X. Zhang, H. Liu, L. Jiang, *Adv. Mater.* **2017**, *29*, 1704253.
[110] J. Liu, X. Zhang, Y. Cui, Y. Liu, W. Wang, Y. Guo, Q. Wang, X. Dong, *ACS Appl. Mater. Interfaces* **2024**, *16*, 5208.
[111] Q. Li, C. Wen, J. Yang, X. Zhou, Y. Zhu, J. Zheng, G. Cheng, J. Bai, T. Xu, J. Ji, S. Jiang, L. Zhang, P. Zhang, *Chem. Rev.* **2022**, *122*, 17073.
[112] J. Yang, N. Cai, H. Zhai, J. Zhang, Y. Zhu, L. Zhang, *Sci. Rep.* **2016**, *6*, 37458.
[113] Q. Shao, S. Jiang, *Adv. Mater.* **2015**, *27*, 15.
[114] J. S. Sperry, D. J. Robson, In *Conifer Cold Hardiness*, F. J. Bigras, S. J. Colombo, Eds. Springer Netherlands, Dordrecht, **2001**, 121.
[115] R. Gupta, R. Deswal, *J. Biosci.* **2014**, *39*, 931.
[116] K. Liu, L. Jiang, *ACS Nano* **2011**, *5*, 6786.
[117] J. Xu, R. Jing, X. Ren, G. Gao, *J. Mater. Chem. A* **2020**, *8*, 9373.
[118] C. Wang, C. G. Wiener, P. I. Sepulveda-Medina, C. Ye, D. S. Simmons, R. Li, M. Fukuto, R. A. Weiss, B. D. Vogt, *Chem. Mater.* **2018**, *31*, 135.
[119] H. Gao, Z. Zhao, Y. Cai, J. Zhou, W. Hua, L. Chen, L. Wang, J. Zhang, D. Han, M. Liu, L. Jiang, *Nat. Commun.* **2017**, *8*, 15911.
[120] X. Li, D. Lou, H. Wang, X. Sun, J. Li, Y.-N. Liu, *Adv. Funct. Mater.* **2020**, *30*, 2007291.
[121] C. Lu, X. Chen, *Nano Lett.* **2020**, *20*, 1907.
[122] K. He, P. Cai, S. Ji, Z. Tang, Z. Fang, W. Li, J. Yu, J. Su, Y. Luo, F. Zhang, T. Wang, M. Wang, C. Wan, L. Pan, B. Ji, D. Li, X. Chen, *Adv. Mater.* **2023**, *36*, 2311255.
[123] H. Yuk, T. Zhang, G. A. Parada, X. Liu, X. Zhao, *Nat. Commun.* **2016**, *7*, 12028.
[124] M. Gori, S. M. Giannitelli, G. Vadala, R. Papalia, L. Zollo, M. Sanchez, M. Trombetta, A. Rainer, G. Di Pino, V. Denaro, *Molecules* **2022**, *27*, 3126.
[125] L. Zhang, Z. Cao, T. Bai, L. Carr, J.-R. Ella-Menye, C. Irvin, B. D. Ratner, S. Jiang, *Nat. Biotechnol.* **2013**, *31*, 553.
[126] L. E. Jansen, L. D. Amer, E. Y. Chen, T. V. Nguyen, L. S. Saleh, T. Emrick, W. F. Liu, S. J. Bryant, S. R. Peyton, *Biomacromolecules* **2018**, *19*, 2880.
[127] M. D. Swartzlander, C. A. Barnes, A. K. Blakney, J. L. Kaar, T. R. Kyriakides, S. J. Bryant, *Biomaterials* **2015**, *41*, 26.
[128] D. Zhang, Q. Chen, W. Zhang, H. Liu, J. Wan, Y. Qian, B. Li, S. Tang, Y. Liu, S. Chen, R. Liu, *Angew. Chem., Int. Ed.* **2020**, *59*, 9586.
[129] Y. Chandorkar, K. Ravikumar, B. Basu, *ACS Biomater. Sci. Eng.* **2019**, *5*, 19.
[130] Y. Wang, F. Papadimitrakopoulos, D. J. Burgess, *J. Control. Rel.* **2013**, *169*, 341.
[131] B. Gu, F. Papadimitrakopoulos, D. J. Burgess, *J. Control. Rel.* **2018**, *289*, 35.
[132] S. N. Pawar, K. J. Edgar, *Biomaterials* **2012**, *33*, 3279.
[133] O. Veiseh, J. C. Doloff, M. Ma, A. J. Vegas, H. H. Tam, A. R. Bader, J. Li, E. Langan, J. Wyckoff, W. S. Loo, S. Jhunjhunwala, A. Chiu, S. Siebert, K. Tang, J. Hollister-Lock, S. Aresta-Dasilva, M. Bochenek, J. Mendoza-Elias, Y. Wang, M. Qi, D. M. Lavin, M. Chen, N. Dholakia, R. Thakrar, I. Lacik, G. C. Weir, J. Oberholzer, D. L. Greiner, R. Langer, D. G. Anderson, *Nat. Mater.* **2015**, *14*, 643.
[134] J. Zhang, Y. Zhu, J. Song, J. Yang, C. Pan, T. Xu, L. Zhang, *ACS Appl. Mater. Interfaces* **2018**, *10*, 6879.
[135] J. Zhang, Y. Zhu, J. Song, T. Xu, J. Yang, Y. Du, L. Zhang, *Adv. Funct. Mater.* **2019**, *29*, 1900140.
[136] A. J. Vegas, O. Veiseh, J. C. Doloff, M. Ma, H. H. Tam, K. Bratlie, J. Li, A. R. Bader, E. Langan, K. Olejnik, P. Fenton, J. W. Kang, J. Hollister-Locke, M. A. Bochenek, A. Chiu, S. Siebert, K. Tang, S. Jhunjhunwala, S. Aresta-Dasilva, N. Dholakia, R. Thakrar, T. Vietti, M. Chen, J. Cohen, K. Siniakowicz, M. Qi, J. McGarrigle, A. C. Graham, S. Lyle, D. M. Harlan, et al., *Nat. Biotechnol.* **2016**, *34*, 345.
[137] S. Liu, R. Zhang, J. Mao, Y. Zhao, Q. Cai, Z. Guo, *Sci. Adv.* **2022**, *8*, eabn5097.
[138] X. Pu, M. Liu, X. Chen, J. Sun, C. Du, Y. Zhang, J. Zhai, W. Hu, Z. L. Wang, *Sci. Adv* **2017**, *3*, e1700015.
[139] Z. Xu, F. Zhou, H. Yan, G. Gao, H. Li, R. Li, T. Chen, *Nat. Energy* **2021**, *90*, 106614.
[140] M. Chen, W. Zhou, A. Wang, A. Huang, J. Chen, J. Xu, C.-P. Wong, *J. Mater. Chem. A* **2020**, *8*, 6828.
[141] J. Wang, Q. Li, K. Li, X. Sun, Y. Wang, T. Zhuang, J. Yan, H. Wang, *Adv. Mater.* **2022**, *34*, 2109904.
[142] Y. Yan, S. Duan, B. Liu, S. Wu, Y. Alsaid, B. Yao, S. Nandi, Y. Du, T. W. Wang, Y. Li, X. He, *Adv. Mater.* **2023**, *35*, 2211673.
[143] H. Yu, N. Rouelle, A. Qiu, J. A. Oh, D. M. Kempaiah, J. D. Whittle, M. Aakyiir, W. Xing, J. Ma, *ACS Appl. Mater. Interfaces* **2020**, *12*, 37977.
[144] T. Liu, M. Liu, S. Dou, J. Sun, Z. Cong, C. Jiang, C. Du, X. Pu, W. Hu, Z. L. Wang, *ACS Nano* **2018**, *12*, 2818.
[145] L. Ma, S. Chen, D. Wang, Q. Yang, F. Mo, G. Liang, N. Li, H. Zhang, J. A. Zapien, C. Zhi, *Adv. Energy Mater.* **2019**, *9*, 1803046.
[146] Z. Liu, D. Wang, Z. Tang, G. Liang, Q. Yang, H. Li, L. Ma, F. Mo, C. Zhi, *Energy Storage Mater.* **2019**, *23*, 636.
[147] X. Jing, H. Li, H.-Y. Mi, P.-Y. Feng, X. Tao, Y. Liu, C. Liu, C. Shen, *J. Mater. Chem. C* **2020**, *8*, 5752.
[148] X. Luo, L. Zhu, Y.-C. Wang, J. Li, J. Nie, Z. L. Wang, *Adv. Funct. Mater.* **2021**, *31*, 2104928.
[149] Y. S. Kim, M. Liu, Y. Ishida, Y. Ebina, M. Osada, T. Sasaki, T. Hikima, M. Takata, T. Aida, *Nat. Mater.* **2015**, *14*, 1002.
[150] X. Liu, J. Liu, S. Lin, X. Zhao, *Mater. Today* **2020**, *36*, 102.
[151] C. Yang, Z. Liu, C. Chen, K. Shi, L. Zhang, X. J. Ju, W. Wang, R. Xie, L. Y. Chu, *ACS Appl. Mater. Interfaces* **2017**, *9*, 15758.
[152] S. Y. Zheng, Y. Shen, F. Zhu, J. Yin, J. Qian, J. Fu, Z. L Wu, Q. Zheng, *Adv. Funct. Mater.* **2018**, *28*, 1803366.
[153] H. Qin, T. Zhang, N. Li, H. P. Cong, S. H. Yu, *Nat. Commun.* **2019**, *10*, 2202.
[154] S. Terryn, J. Langenbach, E. Roels, J. Brancart, C. Bakkali-Hassani, Q.-A. Poutrel, A. Georgopoulou, G. T. Thuruthel, A. Safaei, P. Ferrentino, T. Sebastian, S. Norvez, F. Iida, A. W. Bosman, F. Tournilhac, F. Clemens, G. Van Assche, B. Vanderborght, *Mater. Today* **2021**, *47*, 187.
[155] X. He, S. Yang, C. Liu, T. Xu, X. Zhang, *Adv. Healthcare Mater.* **2020**, *9*, 2000941.
[156] L. Wang, T. Xu, X. He, X. Zhang, *J. Mater. Chem. C* **2021**, *9*, 14938.
[157] L. Wang, T. Xu, X. Zhang, *TrAC, Trends Anal. Chem.* **2021**, *134*, 116130.
[158] Z. Wang, J. Chen, Y. Cong, H. Zhang, T. Xu, L. Nie, J. Fu, *Chem. Mater.* **2018**, *30*, 8062.
[159] E. S. Sani, C. Xu, C. Wang, Y. Song, J. Min, J. Tu, S. A. Solomon, J. Li, J. L. Banks, D. G. Armstrong, W. Gao, *Sci. Adv.* **2023**, *9*, adf7388.
[160] S. Zhang, F. Cicoira, *Adv. Mater.* **2017**, *29*, 1703098.
[161] X. P. Hao, C. W. Zhang, X. N. Zhang, L. X. Hou, J. Hu, M. D. Dickey, Q. Zheng, Z. L Wu, *Small* **2022**, *18*, 2201643.
[162] Z. Li, S. Zhang, Y. Chen, H. Ling, L. Zhao, G. Luo, X. Wang, M. C. Hartel, H. Liu, Y. Xue, R. Haghniaz, K. Lee, W. Sun, H. Kim, J. Lee, Y. Zhao, Y. Zhao, S. Emaminejad, S. Ahadian, N. Ashammakhi, M. R. Dokmeci, Z. Jiang, A. Khademhosseini, *Adv. Funct. Mater.* **2020**, *30*, 2003601.
[163] Y. Jiang, A. A. Trotsyuk, S. Niu, D. Henn, K. Chen, C. C. Shih, M. R. Larson, A. M. Mermin-Bunnell, S. Mittal, J. C. Lai, A. Saberi, E. Beard, S. Jing, D. Zhong, S. R. Steele, K. Sun, T. Jain, E. Zhao, C. R. Neimeth, W. G. Viana, J. Tang, D. Sivaraj, J. Padmanabhan, M. Rodrigues, D. P. Perrault, A. Chattopadhyay, Z. N. Maan, M. C. Leeolou, C. A. Bonham, S. H. Kwon, et al., *Nat. Biotechnol.* **2023**, *41*, 652.

[164] M. Pi, S. Qin, S. Wen, Z. Wang, X. Wang, M. Li, H. Lu, Q. Meng, W. Cui, R. Ran, *Adv. Funct. Mater.* **2022**, *33*, 2210188.
[165] X. Di, J. Hou, M. Yang, G. Wu, P. Sun, *Mater. Horiz.* **2022**, *9*, 3057.
[166] Y. Hu, J. Li, J. Liu, X. Yu, J. Yang, Y. Li, *Sens. Actuat. B: Chem.* **2023**, *378*, 133173.
[167] Q. Liu, A. Chiu, L. Wang, D. An, W. Li, E. Y. Chen, Y. Zhang, Y. Pardo, S. P. McDonough, L. Liu, W. F. Liu, J. Chen, M. Ma, *Biomaterials* **2020**, *230*, 119640.
[168] G. Li, K. Huang, J. Deng, M. Guo, M. Cai, Y. Zhang, C. F. Guo, *Adv. Mater.* **2022**, *34*, 2200261.
[169] C. Cui, C. Fan, Y. Wu, M. Xiao, T. Wu, D. Zhang, X. Chen, B. Liu, Z. Xu, B. Qu, W. Liu, *Adv. Mater.* **2019**, *31*, 1905761.
[170] L. Han, M. Wang, L. O. Prieto-López, X. Deng, J. Cui, *Adv. Funct. Mater.* **2019**, *30*, 1907064.
[171] H. Choi, Y. Kim, S. Kim, H. Jung, S. Lee, K. Kim, H.-S. Han, J. Y. Kim, M. Shin, D. Son, *Nat. Electron.* **2023**, *6*, 779.
[172] Y. Wu, S. Joseph, N. R. Aluru, *J. Phys. Chem. B* **2009**, *113*, 3512.

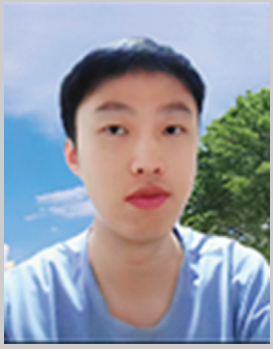

Xuecheng He obtained his Ph.D. in chemistry from the University of Science and Technology Beijing (USTB) in 2022. He once served as a visiting Ph.D. student at Nanyang Technological University (NTU), Singapore, from 2021-2022. Currently, he is working as a postdoctoral research fellow at the University of Hong Kong (HKU), where his research focuses on the development of soft, tough, bioelectronics capable of working under extreme conditions.

Tailin Xu is currently an associate professor at the School of Biomedical Engineering, at Shenzhen University. He obtained his PhD at USTB in 2017. From 2013–2015, he worked as a joint Ph.D. student at the University of California, San Diego (UCSD). His research interests include functional nanoparticles, flexible electronics, and wearable biosensors. Xu works on the editorial board of Frontiers in Bioengineering and Biotechnology (associate editor), Journal of Functional Biomaterials, and Chinese Chemical Letters. Xu was also awarded as the world's Top 2% Scientist (2022,2023).

Shiming Zhang is currently an Assistant Professor at the Department of Electrical and Electronic Engineering (EEE) of HKU, leading the wearable, intelligent, and soft electronics (WISE) research group. Before that, He spent three years at the University of California, Los Angeles (UCLA), as a postdoctoral scholar (group leader on bioelectronics), and obtained his Ph.D. from École Polytechnique, Université de Montréal, Canada, and B.S./M.S. from Jilin University, China. He was recognized as a "Rising Star" by Advanced Science (2022) and an "Emerging Investigator" by Journal of Materials Chemistry C (2022) for his contributions to the interdisciplinary fields of soft semiconductor devices, soft bioelectrochemistry, and hydrogel bioelectronics.